

Electron-phonon hydrodynamics

Xiaoyang Huang^{1,*} and Andrew Lucas^{1,†}

¹*Department of Physics and Center for Theory of Quantum Matter,
University of Colorado, Boulder CO 80309, USA*

(Dated: September 23, 2020)

We develop the theory of hydrodynamics of an isotropic Fermi liquid of electrons coupled to isotropic acoustic phonons, assuming that umklapp processes may be neglected. At low temperatures, the fluid is approximately Galilean invariant; at high temperatures, the fluid is nearly relativistic; at intermediate temperatures, there are seven additional temperature regimes with unconventional thermodynamic properties and hydrodynamic transport coefficients in a three-dimensional system. We predict qualitative signatures of electron-phonon fluids in incoherent transport coefficients, shear and Hall viscosity, and plasmon dispersion relations. Our theory may be relevant for numerous quantum materials where strong electron-phonon scattering has been proposed to underlie a hydrodynamic regime, including WTe₂, WP₂, and PtSn₄.

CONTENTS

1. Introduction	2
2. Summary of results	2
3. Kinetic theory	4
3.1. Formalism	4
3.2. Thermodynamics	6
3.3. Electron-phonon collision integral	6
3.4. Phonon-phonon collision integral	8
4. Hydrodynamics	9
4.1. Speed of sound	10
4.2. Shear viscosity	11
4.3. Bulk viscosity	11
4.4. Incoherent conductivities	12
4.5. Plasmons	14
5. Thermoelectric transport	15
6. Magnetic fields	18
6.1. Viscosity	18
6.2. Magnetotransport	19
7. Conclusion	20
Acknowledgements	21
A. Normalization factor of rotationally invariant basis	21
B. Explicit expressions of electron-phonon relaxation rate	22
1. $T < T_{\text{BG}}$	23
2. $T > T_{\text{BG}}$	23
C. Matrix elements of collision integrals without magnetic field	24

* xiaoyang.huang@colorado.edu

† andrew.j.lucas@colorado.edu

1. INTRODUCTION

The hydrodynamics of correlated electron liquids, theorized many decades ago [1], has recently become increasingly observable in experiments in a broad range of materials, including graphene [2–10] and GaAs [11, 12]; see [13] for a recent review, and [14–21] for recent theoretical developments. More speculatively, proposed evidence for hydrodynamics has been put forth in WTe_2 [22], WP_2 [23–25], PtSn_4 [26] and PdCoO_2 [27, 28]. In these more complicated material systems, the electron’s Fermi surface is highly anisotropic (and may be multiple-sheeted), and electron-phonon coupling cannot be neglected. Can exotic hydrodynamics arise in these material systems, with phenomenology beyond the canonical (Galilean-invariant) hydrodynamics?

To begin to address this question, we revisit the hydrodynamics of a coupled fluid of electrons and acoustic phonons, in more than one spatial dimension $d > 1$. This problem has arisen in the older solid-state literature [29–31], with a recent work [32] revisiting this theory in light of more recent developments. The focus of this earlier literature is largely on low temperature dynamics. The purpose of this paper is to show that there are at least 7 distinct temperature regimes of coupled electron-phonon fluids, exhibiting qualitatively distinct behaviors, that can arise at temperatures below the Fermi temperature in $d = 2$, and at least 9 different temperature regimes in $d > 2$. These distinct temperature regimes arise even with the simplest electron-phonon scattering integrals, and ignoring a multitude of possible microscopic effects such as optical phonon scattering, anisotropy or multi-sheeted Fermi surfaces. These distinct temperature regimes are distinguishable when the ratio of the phonon velocity and the Fermi velocity is parametrically small. In practice, this ratio might typically be around 0.01 to 0.1, which is small enough to distinguish at least a few of the different fluids we will describe (though distinguishing all 9 regimes cleanly would be difficult in principle and in practice). The previous literature [29–32] (as far as we could tell) studies only one of these temperature regimes, that arises at the very lowest temperatures. However, this may not be the range of temperatures most relevant for experiments in many of the material systems listed above.

2. SUMMARY OF RESULTS

We now broadly summarize our results. We first introduce the model of interest. We consider an isotropic and weakly interacting electron Fermi liquid, with an isotropic dispersion relation. We suppose that the Fermi temperature is T_F , the Fermi momentum is p_F , and the Fermi velocity is v_F . We assume the electronic density of states at the Fermi energy is given by

$$\nu = \frac{\partial n}{\partial \mu} = \frac{\Omega_{d-1}}{(2\pi)^d} d p_F^{d-1} \frac{\partial p_F}{\partial \mu} = d \frac{n}{v_F p_F} = \frac{dn}{m v_F^2} \sim \frac{p_F^{d-1}}{v_F}. \quad (2.1)$$

where Ω_{d-1} is the area of the unit sphere in $d - 1$ dimensions and m is an effective quasiparticle mass. Working in units where $k_B = 1$, the single-particle fermion dispersion relation near the Fermi surface is

$$\epsilon(\mathbf{p}) = T_F + v_F(|\mathbf{p}| - p_F) + \frac{\partial_p v_F}{2} (|\mathbf{p}| - p_F)^2 + \dots \quad (2.2)$$

Similarly, we consider isotropic acoustic phonons whose frequency is given by

$$\omega(\mathbf{p}) = v_{\text{ph}} |\mathbf{p}|. \quad (2.3)$$

We restrict our calculations to temperatures $T \ll T_F$, and will generally suppress all subleading corrections in the small parameter T/T_F except where stated. In usual metals ($T_F \sim 10000$ K) the criterion is impossible to violate, but for low density systems it is possible, e.g. in graphene [3, 6] and GaAs [12, 33, 34]. The system we consider is d -dimensional with $d > 1$. Experimental systems exist with both $d = 2$ (exactly, or approximately) and $d = 3$.

There are three dimensionless numbers that will prove particularly important in our analysis. First, there is the small parameter

$$\bar{a} \equiv \frac{a}{p_F} \equiv \frac{\pi T}{\sqrt{3} p_F v_F}, \quad (2.4)$$

T	$< T_1$	T_1 to T_2	T_2 to T_3	T_3 to T_4	T_4 to T_{BG}	T_{BG} to T_6	T_6 to T_7	T_7 to T_8	T_8 to T_{F}
regime	I	II	III	IV	V	VI	VII	VIII	IX
sound velocity	v_{F}/\sqrt{d}				$v_{\text{F}}/\bar{w}\sqrt{d}$		v_{ph}/\sqrt{d}		
charge current	coherent ($ J_{\text{inc}} \propto \bar{a}$)		coherent ($ J_{\text{inc}} \propto \bar{w}$)		incoherent				
heat current	incoherent							coherent	
energy current	coherent				incoherent				coherent
electron scattering	small angle					large angle			
bulk viscosity	by $ 2\rangle_{\text{e}}$		by $ 1\rangle_{\text{ph}}$		by $ 1\rangle_{\text{e}}$				
Σ v.s. η	$\Sigma < \eta$				$\Sigma > \eta$				

TABLE 1. A summary of the hydrodynamic properties of a coupled electron-phonon fluid. The ratio r is defined in (2.6) and the temperature crossovers are defined in (2.8).

which represents the smallness of thermal fluctuations of the electrons about their Fermi surface – specifically, the enhancement of the momentum carried by thermal fluctuations of electrons. Secondly, we have the ratio

$$\bar{w} \equiv \frac{w}{p_{\text{F}}\sqrt{\nu/2}} \equiv \frac{I(d)}{p_{\text{F}}\sqrt{\nu/2}} \sqrt{\frac{T^{d+1}}{v_{\text{ph}}^{d+2}}}, \quad (2.5)$$

where $I(d)$ is a dimensionless number defined in (A2). \bar{w} represents the ratio of the momentum carried by phonons to momentum carried by electrons in equilibrium. As \bar{w} becomes larger with increasing temperature, the fluid's properties qualitatively change. $\bar{w} \ll 1$ and $\bar{w} \gg 1$ are both limits which can be achieved in experimental devices, as we will soon see. Finally, there is the small ratio

$$r = \frac{v_{\text{ph}}}{v_{\text{F}}} \quad (2.6)$$

characterizing the small ratio of quasiparticle velocities between phonons and electrons. We assume that the dispersion relation is sufficiently simple so that $T_{\text{F}} \sim p_{\text{F}}v_{\text{F}}$, in which case we also obtain the following useful scaling relation:

$$\bar{w} \sim \left(\frac{T}{T_{\text{F}}}\right)^{(d+1)/2} r^{-(d+2)/2} \sim \frac{\bar{a}^{(d+1)/2}}{r^{(d+2)/2}}. \quad (2.7)$$

The main result of this paper is the calculation of hydrodynamic transport coefficients in electron-phonon hydrodynamics. We summarize the results in Table 1. As a function of temperature T , in $d > 2$ spatial dimensions there is a zoo of temperature scales at which certain properties change, which we list below:

$$T_1 = r^{\frac{d+2}{d-1}} T_{\text{F}}, \quad (2.8a)$$

$$T_2 = r^{\frac{d-1}{d-2}} T_{\text{F}}, \quad (2.8b)$$

$$T_3 = r^{\frac{d}{d-1}} T_{\text{F}}, \quad (2.8c)$$

$$T_4 = r^{\frac{d+2}{d+1}} T_{\text{F}}, \quad (2.8d)$$

$$T_5 = T_{\text{BG}} = rT_{\text{F}}, \quad (2.8e)$$

$$T_6 = r^{\frac{d}{d+1}} T_{\text{F}}, \quad (2.8f)$$

$$T_7 = r^{\frac{d-2}{d-1}} T_{\text{F}}, \quad (2.8g)$$

$$T_8 = r^{\frac{d-2}{d+1}} T_{\text{F}}. \quad (2.8h)$$

When temperature is low enough ($T < T_1$), the phonon modes essentially become irrelevant, except for providing a scattering mechanism for the electrons. This is the regime studied in previous papers [29, 32].

However, above temperature T_1 , the phonons begin to play a more interesting role. For the discussion that follows, let us assume the ballpark estimates $T_{\text{F}} \sim 10000$ K and $r \approx 0.03$, and consider a metal in $d = 3$. In this cartoon metal, $T_1 \sim 2$ K. When $T > T_1$, the phonons begin to dominate the incoherent part of the charge conductivity, which now becomes anomalously large, even for an isotropic fluid.¹ However, in an isotropic fluid, the effect will be fairly small.

¹ Note that in an anisotropic fluid [28], the incoherent conductivity will be large even in the lower temperature regimes, in which case this temperature scale becomes more dramatic.

At temperature T_2 (about 10 K), the bulk viscosity becomes dominated by phonons, although again the correction is quite small. At T_3 (about 60 K) and beyond, the bulk viscosity becomes dominated by electrons again, but is not suppressed for any electronic dispersion relation.²

The fluid completely begins to change its character at T_4 (in our cartoon, about 140 K). At this temperature, $\bar{w} \sim 1$, and so the momentum of the coupled fluid begins to become phonon-dominated. This leads to a number of crucial changes, including a rapid *decrease* in the sound speed ($v_s \sim T^{-(d+1)/2}$), a large incoherent electrical conductivity, and a sound mode whose decay is dominated by incoherent conductivity rather than viscosity. As we describe later, such changes may be visible in experiments by studying changes to the plasmon dispersion relation. At $T_5 = T_{\text{BG}}$, the Bloch-Grüneisen temperature,³ there are surprisingly few changes to the hydrodynamic properties of the fluid, beyond a possible sharp decrease in the shear viscosity. In our numerical cartoon, $T_{\text{BG}} \sim 300$ K is room temperature.

The final dramatic change arises at temperature T_6 (about 800 K in our cartoon), where the phonons dominate the sound mode, which now propagates at its high temperature velocity of

$$v_s = \frac{v_{\text{ph}}}{\sqrt{d}}. \quad (2.9)$$

At temperature T_7 (about 1800 K in our cartoon), the heat current becomes approximately coherent; at temperature T_8 (about 4000 K in our cartoon) the energy current becomes coherent. Once the energy current becomes coherent, the hydrodynamics of the coupled electron-phonon fluid becomes essentially a nearly charge neutral relativistic fluid [36]: the energy current and momentum density are approximately equivalent, and the charge current is incoherent while the energy/heat currents are nearly coherent. Interestingly enough, the speed of sound of the fluid is also compatible with a conformal fluid, since at high temperatures v_{ph} plays the role of an approximate speed of light for the dominant species. However, the fluid has the largest bulk viscosity at these high temperatures, so it is not ultimately a conformal fluid, even approximately [37].

In Section 5, we review the thermoelectric transport properties of an electron-phonon fluid in the presence of momentum relaxation [38], in light of the 8 different temperature scales described in (2.8). Although the precise temperature scales at which the WF law fails are sensitive to the precise rates of momentum relaxation, we will give a qualitative overview of how the different temperature scales in (2.8) arise in the Lorenz ratio, and how the thermal and electrical conductivity are sensitive to the complicated thermodynamics and incoherent conductivities described above. Since typical electron-phonon fluids exhibit violations of the Wiedemann-Franz Law just below T_{BG} and many of the signatures of electron-phonon hydrodynamics in materials such as WP_2 and PtSn_4 arises at temperatures just as L dips below L_0 , it may be reasonable to estimate many electron-phonon fluids as being in the temperature regime $T_4 < T < T_{\text{BG}}$ (though of course, this is a quite heuristic observation). We hope, therefore, that many of the exotic hydrodynamic phenomena described above could (in principle) be observable. For example, in thin films, the exotic sound speed might be observable by careful studies of the temperature dependence of the real part of plasmon dispersion relations, as we will describe in Section 4.5. The imaginary part of the plasmon dispersion relation also will obtain (in two dimensions) a highly unusual imaginary part [39] arising from the large incoherent conductivity.

In Section 6, we briefly describe hydrodynamics and transport of the electron-phonon fluid in a background magnetic field. For simplicity we focus on the case of two dimensional systems. Depending on microscopic details of phonon-phonon scattering, the relationship between shear viscosity and Hall viscosity can either mirror a conventional Fermi liquid with negligible electron-phonon scattering [40] or appear rather unconventional.

3. KINETIC THEORY

In this section, we review a general formalism to solve the transport problem. Our notation follows [41–43].

3.1. Formalism

Consider a Fermi liquid with weak interactions. For the moment, let us imagine a single species of particle – we will relax this shortly. We can describe transport by determining the response of the distribution function $f(\mathbf{x}, \mathbf{p})$, which can roughly be interpreted as the number of quasiparticles of momentum \mathbf{p} near the spatial point \mathbf{x} . Since

² If the electrons had $\epsilon \propto p^2$, then the bulk viscosity (in the absence of phonons carrying momentum) exactly vanishes. For $T < T_1$ this implies the bulk viscosity is much smaller than it would be for a generic Fermi liquid. Admittedly, this effect is very hard to see experimentally; this is simply an interesting theoretical observation.

³ The Bloch-Grüneisen temperature T_{BG} arises when the phonon-limited resistivity shows a dramatic change from $\rho \sim T^{d+2}$ to $\rho \sim T$ [35] (in the absence of phonon drag, at least). It can be understood from the bosonic nature of phonon modes: when $T < T_{\text{BG}}$, the volume of phonon momentum integration is restricted to the T/v_{ph} window; when $T > T_{\text{BG}}$, the phonons are more like a classical gas with equipartition distribution.

these quasiparticles are assumed to be long-lived, this interpretation is sensible. The evolution of f is governed by the Boltzmann equation [44]:

$$\partial_t f + \mathbf{v}_{\mathbf{p}} \cdot \partial_{\mathbf{x}} f + \mathbf{F}_{\text{ext}} \cdot \partial_{\mathbf{p}} f = \mathcal{C}[f], \quad (3.1)$$

where

$$\mathbf{v}_{\mathbf{p}} = \partial_{\mathbf{p}} \epsilon_{\mathbf{p}} \quad (3.2)$$

is the quasiparticle velocity, \mathbf{F}_{ext} is the external force, and $\mathcal{C}[f]$ accounts for the multi-particle scattering events arising due to interactions between quasiparticles. We assume the electron band $\epsilon_{\mathbf{p}}$ to be inversion symmetric and time reversal symmetric and neglect the spin degree of freedom for simplicity. We write

$$f(\mathbf{x}, \mathbf{p}) = f_0(\mathbf{x}, \mathbf{p}) + \delta f(\mathbf{x}, \mathbf{p}) \equiv f_0(\mathbf{x}, \mathbf{p}) + \left(-\frac{\partial f}{\partial \epsilon} \right) \Phi(\mathbf{x}, \mathbf{p}), \quad (3.3)$$

where f_0 is the equilibrium distribution function, and δf is the infinitesimal correction due to the deviation from equilibrium. Within linear response, (3.1) reduces to

$$\partial_t \delta f + \mathbf{v}_{\mathbf{p}} \cdot \partial_{\mathbf{x}} \delta f + \delta \mathbf{F}_{\text{ext}} \cdot \partial_{\mathbf{p}} f_0 = \delta \mathcal{C}[\delta f] \quad (3.4)$$

where the right hand side is, in general, a non-local function in \mathbf{p} . The external force is given by

$$\delta \mathbf{F}_{\text{ext}} = -e \delta \mathbf{E} + (\epsilon - \mu) \frac{\nabla \delta T}{T} \quad (3.5)$$

and arises due to external electric fields and temperature gradients.

We interpret $\Phi(\mathbf{x}, \mathbf{p})$ as a vector, with the \mathbf{p} dependence abstracted into Dirac bra-ket notation. Hence, we write

$$|\Phi\rangle = \int d^d p \Phi(\mathbf{x}, \mathbf{p}) |\mathbf{p}\rangle, \quad (3.6)$$

and define the inner product

$$\langle \mathbf{p} | \mathbf{p}' \rangle = \left(-\frac{\partial f}{\partial \epsilon} \right) |_{\mathbf{p}} \frac{\delta(\mathbf{p} - \mathbf{p}')}{(2\pi\hbar)^d}. \quad (3.7)$$

The charge and thermal current, when evaluated on a given distribution function f , can be written as inner products

$$J_i(\mathbf{x}) = \langle \Phi | J_i \rangle = -e \int \frac{d^d p}{(2\pi\hbar)^d} v_i \left(-\frac{\partial f}{\partial \epsilon} \right) \Phi(\mathbf{x}, \mathbf{p}), \quad |J_i\rangle \equiv -e \int d^d p v_i(\mathbf{p}) |\mathbf{p}\rangle, \quad (3.8a)$$

$$Q_i(\mathbf{x}) = \langle \Phi | Q_i \rangle = \int \frac{d^d p}{(2\pi\hbar)^d} (\epsilon - \mu) v_i \left(-\frac{\partial f}{\partial \epsilon} \right) \Phi(\mathbf{x}, \mathbf{p}), \quad |Q_i\rangle \equiv \int d^d p (\epsilon - \mu) v_i(\mathbf{p}) |\mathbf{p}\rangle, \quad (3.8b)$$

since in equilibrium there is no charge or heat current. We define the linearized collision integral W to be the map in the vector space $W : |\mathbf{p}\rangle \rightarrow |\mathbf{p}'\rangle$ giving the linearized collision integral

$$\delta \mathcal{C}_{\mathbf{p}} = \langle \mathbf{p} | W | \Phi \rangle. \quad (3.9)$$

The linearized Boltzmann equation becomes

$$\partial_t |\Phi\rangle + \mathbf{v}_{\mathbf{p}} \cdot \partial_{\mathbf{x}} |\Phi\rangle - E_i |J_i\rangle + \frac{\nabla_i T}{T} |Q_i\rangle = -W |\Phi\rangle. \quad (3.10)$$

We remind readers that the equilibrium distribution for the fermionic electronic quasiparticles is

$$f_{\text{F}}^0(\mathbf{p}) = \frac{1}{1 + e^{\beta(\epsilon(\mathbf{p}) - \mu)}}, \quad (3.11)$$

while for the bosonic acoustic phonons it is

$$f_{\text{B}}^0(\mathbf{p}) = \frac{1}{e^{\beta\omega(\mathbf{p})} - 1}. \quad (3.12)$$

The velocity of the electrons is

$$\mathbf{v}_{\mathbf{p}} = \partial_{\mathbf{p}} \epsilon_{\mathbf{p}} = v_{\text{F}} \frac{\mathbf{p}}{|\mathbf{p}|} \quad (3.13)$$

and the velocity of the phonons is

$$\mathbf{v}_{\mathbf{p}} = \partial_{\mathbf{p}} \omega(\mathbf{p}) = v_{\text{ph}} \frac{\mathbf{p}}{|\mathbf{p}|}. \quad (3.14)$$

3.2. Thermodynamics

We assume that the system is rotationally invariant, i.e. both the dispersion relation and collision integral are rotationally invariant. Then, a convenient basis could be applied

$$|\tilde{n}, \mathbf{m}\rangle_e = \int d^d p (p - p_F)^n Y_{\mathbf{m}}(\theta_1, \dots, \theta_{d-1}) |\mathbf{p}\rangle, \quad |\tilde{n}, \mathbf{m}\rangle_{\text{ph}} = \int d^d q q^n Y_{\mathbf{m}}(\theta_1, \dots, \theta_{d-1}) |\mathbf{q}\rangle, \quad (3.15)$$

where $Y_{\mathbf{m}}$ is the spherical harmonics with ‘‘angle’’ $\mathbf{m} = (m_1, \dots, m_{d-1})$. In the above equation, and henceforth, $p = |\mathbf{p}|$, $\theta_1, \dots, \theta_{d-1}$ indicate the angular coordinates of \mathbf{p} , and we will use two-dimensional spherical harmonic $Y_m = e^{im\theta}$ for illustration in the rest of this subsection. The generalization to higher dimension is straightforward. The ‘‘angle’’ indices are omitted when indicating typical relaxation rate from then on. However, these basis vectors are not normalized in the radial direction, so we use the standard Gram-Schmidt method to obtain an orthonormal basis $|n, m\rangle_{e,\text{ph}}$, denoted with no tildes. The most important normalization factors are listed below (see Appendix A):

$$\langle \tilde{0}, m' | \tilde{0}, m \rangle_e = \nu \delta_{m,m'}, \quad (3.16a)$$

$$\langle \tilde{1}, m' | \tilde{1}, m \rangle_e = \nu a^2 \delta_{m,m'}, \quad (3.16b)$$

$$\langle \tilde{1}, m' | \tilde{1}, m \rangle_{\text{ph}} = 2w^2 \delta_{m,m'}. \quad (3.16c)$$

In our example of $d = 2$, we can write the total momentum, the charge current and the thermal current as

$$|p_x\rangle \pm i|p_y\rangle = p_F |\tilde{0}, \pm 1\rangle_e + |\tilde{1}, \pm 1\rangle_e + |\tilde{1}, \pm 1\rangle_{\text{ph}}, \quad (3.17a)$$

$$|J_x\rangle \pm i|J_y\rangle = -e(v_F |\tilde{0}, \pm 1\rangle_e + \partial_p v_F |\tilde{1}, \pm 1\rangle_e + \dots), \quad (3.17b)$$

$$|Q_x\rangle \pm i|Q_y\rangle = v_F^2 |\tilde{1}, \pm 1\rangle_e + \dots + v_{\text{ph}}^2 |\tilde{1}, \pm 1\rangle_{\text{ph}}. \quad (3.17c)$$

The momentum operator is exact while the current operators are only written to leading order in T/T_F . Besides, the energy density vector $|\epsilon\rangle$ and charge density vector $|\rho\rangle$ are given by

$$|\epsilon\rangle = \mu |\rho\rangle + |\tilde{\epsilon}\rangle = \mu |\tilde{0}, 0\rangle_e + v_F |\tilde{1}, 0\rangle_e + v_{\text{ph}} |\tilde{1}, 0\rangle_{\text{ph}} + \dots, \quad (3.18)$$

where $|\tilde{\epsilon}\rangle$ is the energy density part orthogonal to density. Based on above identities, important thermodynamic properties including momentum susceptibility M (mass density in a Galilean-invariant fluid), specific heat c , charge density ρ and energy density ϵ could be calculated explicitly,

$$M \equiv \langle p_x | p_x \rangle = \frac{\nu}{2} p_F^2 (1 + \bar{a}^2 + \bar{w}^2), \quad (3.19a)$$

$$c = T \partial_T \epsilon = \langle \tilde{\epsilon} | \tilde{\epsilon} \rangle = \frac{\nu}{2} v_F^2 p_F^2 (\bar{a}^2 + r^2 \bar{w}^2 + \dots), \quad (3.19b)$$

$$\rho \equiv \frac{\langle J_x | p_x \rangle}{-e} = \frac{\nu}{2} v_F p_F (1 + (p_F \partial_p \ln v_F) \bar{a}^2 + \dots), \quad (3.19c)$$

$$\epsilon \equiv \frac{\langle Q_x | p_x \rangle}{T} = \frac{\nu}{2T} v_F^2 p_F^2 (\bar{a}^2 + r^2 \bar{w}^2 + \dots). \quad (3.19d)$$

3.3. Electron-phonon collision integral

We now describe the collision integrals, beginning with the electron-phonon interactions. The dominant such interaction is a single phonon emission/absorption event [32, 45]:

$$H_{e\text{-ph}} = \sum A_{\mathbf{q}, \mathbf{k}_1, \mathbf{k}_2} (a_{\mathbf{q}} + a_{-\mathbf{q}}^\dagger) c_{\mathbf{k}_1}^\dagger c_{\mathbf{k}_2}, \quad (3.20)$$

The Boltzmann equations for electrons and phonons are

$$\partial_t f_{\text{F}} + \mathbf{v}_{\text{F}} \cdot \partial_{\mathbf{x}} f_{\text{F}} + \mathbf{F} \cdot \nabla_{\mathbf{p}} f_{\text{F}} = \mathcal{C}_{\text{e-ph}}, \quad (3.21a)$$

$$\partial_t f_{\text{B}} + \mathbf{v}_{\text{ph}} \cdot \partial_{\mathbf{x}} f_{\text{B}} + \mathbf{F} \cdot \nabla_{\mathbf{p}} f_{\text{B}} = \mathcal{C}_{\text{ph-e}}, \quad (3.21b)$$

where

$$\mathcal{C}_{\text{e-ph}} = \int d^d \mathbf{q} d^d \mathbf{k}_1 |A|^2 \delta(\mathbf{k}_2 - \mathbf{k}_1 - \mathbf{q}) \delta(\epsilon_{k_2} - \epsilon_{k_1} - \omega_q) \{f_{\text{F}k_1}(1 - f_{\text{F}k_2})f_{\text{B}q} - f_{\text{F}k_2}(1 - f_{\text{F}k_1})(1 + f_{\text{B}q})\}. \quad (3.22)$$

$\mathcal{C}_{\text{ph-e}}$ is given by the same equation but with an integral over $\mathbf{k}_1, \mathbf{k}_2$. In the long-wavelength limit, the transition probability is approximated by [46]

$$|A|^2 \sim D_{\text{e-ph}} |\mathbf{q}|. \quad (3.23)$$

Following (3.3), we are able to linearize the Boltzmann equation (see explicit derivation in Appendix B)

$$\langle \Phi | W_{\text{e-ph}} | \Phi \rangle = \beta \int d^d \mathbf{q} d^d \mathbf{k}_1 d^d \mathbf{k}_2 |A|^2 \delta(\mathbf{k}_2 - \mathbf{k}_1 - \mathbf{q}) \delta(\epsilon_{k_2} - \epsilon_{k_1} - \omega_q) (1 - f_{\text{F}k_2}) f_{\text{F}k_1} f_{\text{B}q} |\Phi_{k_1} - \Phi_{k_2} + \Phi_q|^2. \quad (3.24)$$

However, after linearization, (3.21) are still coupled integrodifferential equations which are difficult to solve analytically. Nevertheless, a typical relaxation rate is good enough to estimate the scalings of overall prefactors of hydrodynamics and thermodynamic properties of thermoelectric transport. To obtain the typical scattering rate for electron (phonon) modes, we set the Ansatz $\Phi_{\text{ph}} = 0$ ($\Phi_{\text{e}} = 0$). We summarize the results here, and refer readers to the explicit calculations in Appendix B:

$$\gamma_{\text{e}} = \langle 0 | W_{\text{e-ph}} | 0 \rangle_{\text{e}} = \begin{cases} \gamma & T < T_{\text{BG}} \\ \bar{\gamma} & T_{\text{BG}} < T \ll T_{\text{F}} \end{cases}, \quad (3.25a)$$

$$\gamma'_{\text{e}} = \langle 1 | W_{\text{e-ph}} | 1 \rangle_{\text{e}} = \begin{cases} \gamma r^2 / \bar{a}^2 & T < T_{\text{BG}} \\ \bar{\gamma} & T_{\text{BG}} < T \ll T_{\text{F}} \end{cases}, \quad (3.25b)$$

$$\gamma_{\text{ph}} = \langle 1 | W_{\text{e-ph}} | 1 \rangle_{\text{ph}} = \begin{cases} \gamma / \bar{w}^2 & T < T_{\text{BG}} \\ \bar{\gamma} / \bar{w}^2 & T_{\text{BG}} < T \ll T_{\text{F}} \end{cases}, \quad (3.25c)$$

where γ and $\bar{\gamma}$ are celebrated electron-phonon scattering rates separated by Bloch-Grüneisen temperature [35]:

$$\gamma = \alpha^2 (2) \frac{2}{\nu p_{\text{F}}^2} T^{d+2} \sim \gamma_0 \left(\frac{T}{T_{\text{BG}}} \right)^{d+1} \left(\frac{T}{T_{\text{F}}} \right) \propto T^{d+2}, \quad (3.26a)$$

$$\bar{\gamma} = \alpha'^2 (2) \frac{2}{\nu p_{\text{F}}^2} T \sim \gamma_0 \left(\frac{T}{T_{\text{F}}} \right) \propto T, \quad (3.26b)$$

where

$$\gamma_0 = D_{\text{e-ph}} \frac{p_{\text{F}}^d}{v_{\text{ph}}}. \quad (3.27)$$

So far, the results are exact, and they consist of diagonal terms of the collision integral. To account for the momentum conservation, we multiply the collision integral with projectors:

$$W'_{\text{e-ph}} = (\mathbb{1} - \mathbb{P}) W_{\text{e-ph}} (\mathbb{1} - \mathbb{P}), \quad \mathbb{P} = \frac{|p_x\rangle \langle p_x|}{\langle p_x | p_x \rangle}. \quad (3.28)$$

The explicit expression can be found in Appendix C by ignoring impurity scattering there. The projector above has two physical meanings: first, it makes the total momentum a null vector of the collision integral, i.e. the total momentum has no relaxation; second, the projector gives (approximately) off-diagonal terms of the collision integral by mixing the diagonal terms, taking into account the fact that either electron or phonon momentum could be transferred to each other through electron-phonon scattering even if the total momentum is conserved. Nevertheless, thanks to the semi-positivity of the collision integral (given directly by the second-law of thermodynamics), the off-diagonal terms cannot be qualitatively important, that is, using diagonal terms is good enough to determine the scaling in hydrodynamics.

3.4. Phonon-phonon collision integral

When the temperature is greater than the Bloch-Grüneisen temperature T_{BG} , high momentum phonon modes $q > p_{\text{F}}$ are allowed to appear in electron phonon fluid. However, if there is only electron-phonon interaction, they effectively cannot be scattered via the coupling in (3.20) due to the simultaneous momentum conservation and energy conservation (no two electrons can be connected by such a large momentum transfer). A priori, this might seem to lead to the conclusion that there is some non-interacting part of phonon modes that does not participate in hydrodynamics, at least until higher order scattering processes are considered. Another practical solution is simply to account for phonon-phonon scattering processes. For simplicity, we also ignore umklapp phonon-phonon processes, so that momentum remains exactly conserved in the absence of impurities. In what follows, we analyze the phonon-phonon interaction schematically. Our primary goal is to show that the phonon-phonon interaction will couple high energy phonons to low energy phonons, and hence not lead to any additional long-lived degrees of freedom in the hydrodynamic description.

Due to the relativistic dispersion relation of acoustic phonon modes, momentum and energy conservation together imply fast collinear scattering [13, 47]. To see this explicitly, we take a “random” ansatz in phonon subspace

$$|\Phi\rangle = \int d^d q |q\rangle_{\text{ph}}, \quad \langle\Phi|\Phi\rangle \sim r^d \left(\frac{T}{T_{\text{F}}}\right)^{d-1}. \quad (3.29)$$

The first order phonon-phonon interaction

$$H_{\text{ph-ph}} = \sum_{\mathbf{q}, \mathbf{k}} U(\mathbf{q}, \mathbf{k}) a_{\mathbf{q}+\mathbf{k}}^\dagger a_{\mathbf{q}} a_{\mathbf{k}} + \text{h.c.} \quad (3.30)$$

gives rise to the linearized collision integral under the “random” Ansatz

$$\begin{aligned} \langle\Phi|W_{\text{ph-ph}}|\Phi\rangle &= \int d^d q_1 d^d q_2 d^d q_3 |U|^2 \delta(\mathbf{q}_1 - \mathbf{q}_2 - \mathbf{q}_3) \delta(|\mathbf{q}_1| - |\mathbf{q}_2| - |\mathbf{q}_3|) \frac{1}{v_{\text{ph}}} \beta f_{\text{B}q_1} (1 + f_{\text{B}q_2}) (1 + f_{\text{B}q_3}) \\ &= \int^{T/v_{\text{ph}}} d^d q_2 d^d q_3 \delta(|\mathbf{q}_2 + \mathbf{q}_3| - |\mathbf{q}_2| - |\mathbf{q}_3|) \frac{T^2 D_{\text{ph}}}{v_{\text{ph}}^4}, \end{aligned} \quad (3.31)$$

where we have noted that the phonon-phonon interaction typically takes the form [46]

$$|U|^2 \sim D_{\text{ph}} |\mathbf{q}_1| |\mathbf{q}_2| |\mathbf{q}_3|. \quad (3.32)$$

Obviously, the δ -function is only satisfied when the momenta stay parallel, i.e. realizing collinear scattering. Schematically, we denote the high momentum phonon modes ($q > p_{\text{F}}$) and low momentum phonon modes ($q < p_{\text{F}}$) to be $|\text{H}\rangle_{\text{ph}}$ and $|\text{L}\rangle_{\text{ph}}$ (normalized). Since collinear scattering preserves momentum, it cannot relax the phonon momentum, but can mix $|\text{L}\rangle_{\text{ph}}$ and $|\text{H}\rangle_{\text{ph}}$ effectively. We identify the typical relaxation rate for $|\text{H}\rangle_{\text{ph}}$ to relax to $|\text{L}\rangle_{\text{ph}}$ as the collinear scattering rate $\gamma_{\text{ph-ph, coll}} = \langle\Phi|W_{\text{ph-ph, coll}}|\Phi\rangle / \langle\Phi|\Phi\rangle$. Let

$$\mathbf{q}_2 = (q_2, 0), \quad \mathbf{q}_3 = (q_3, \mathbf{q}_\perp) \quad (3.33)$$

where we assume $\mathbf{q}_{2\perp} = 0$ and $\mathbf{q}_{3\perp} \equiv \mathbf{q}_\perp \ll q_{2,3}$ for collinear scattering. Then the delta function in (3.31) becomes

$$\delta(|\mathbf{q}_2 + \mathbf{q}_3| - |\mathbf{q}_2| - |\mathbf{q}_3|) = 2\delta\left(\frac{q_\perp^2}{q_2 + q_3} - \frac{q_\perp^2}{q_3}\right) = \frac{2(q_2 + q_3)q_3}{q_2} \delta(q_\perp^2). \quad (3.34)$$

The collision integral is estimated through

$$\langle\Phi|W_{\text{ph-ph, coll}}|\Phi\rangle = \int^{T/v_{\text{ph}}} dq_2 dq_3 \frac{2(q_2 + q_3)q_3}{q_2} \frac{T^2 D_{\text{ph}}}{v_{\text{ph}}^4} \int d^{d-1} q_\perp q_\perp^{-1} \delta(q_\perp) \sim r^{-7} \left(\frac{T}{T_{\text{F}}}\right)^5 \times \begin{cases} \log(1/\alpha) & d = 2 \\ \text{const.} & d > 2 \end{cases}, \quad (3.35)$$

where the integral has a logarithm divergence in $d = 2$ [47] with $\alpha \rightarrow 0$ the cutoff from self-energy correction [48]. It is known as collinear scattering singularity [13], which is not truly divergent as long as the scattering amplitude $|U|^2$ vanishes for collinear scattering. Then the collinear scattering rate is given by $\gamma_{\text{ph-ph, coll}} \approx T \times A_{\text{ph-ph, coll}}$ with

$$A_{\text{ph-ph, coll}} \approx D_{\text{ph}} \frac{v_{\text{ph}}^{d-7}}{T^{d-5}} \quad (3.36)$$

T	$< T_3$	T_3 to T_4	T_4 to T_{BG}	T_{BG} to T_{F}
scalings	$\gamma_e = \gamma \sim T^{d+2}$, $\gamma'_e = \gamma r^2 / \bar{a}^2 \sim v_{\text{ph}}^2 T^d$, $\gamma_{\text{ph}} = \gamma / \bar{w}^2 \sim v_{\text{ph}}^{d+2} T$	$\gamma_e = \gamma'_e = \bar{\gamma} \sim T$, $\gamma_{\text{ph}} = \bar{\gamma} / \bar{w}^2 \sim v_{\text{ph}}^{d+2} T^{-d}$		
relations	$\gamma_e < \gamma'_e < \gamma_{\text{ph}}$	$\gamma_e < \gamma_{\text{ph}} < \gamma'_e$	$\gamma_{\text{ph}} < \gamma_e < \gamma'_e$	$\gamma_{\text{ph}} < \gamma_e = \gamma'_e \ll \gamma_{\text{ph-ph}}$

TABLE 2. Summary of scattering rate in different temperature regimes. $\gamma_{\text{ph-ph}}$ is a short hand for phonon-phonon scattering rate.

being the dimensionless parameter characterizing the typical amplitude of the collinear phonon-phonon scattering. For $T > T_{\text{BG}}$, we can also write the electron-phonon scattering rate for phonon modes as $\gamma_{e\text{-ph}} \approx T \times A_{e\text{-ph}}$ with

$$A_e \approx D_{e\text{-ph}} \frac{2p_{\text{F}}^{2(d-1)}}{\nu v_{\text{F}}^2} \frac{1}{v_{\text{ph}}}, \quad A_{\text{ph}} \approx D_{e\text{-ph}} \frac{p_{\text{F}}^{2d} v_{\text{ph}}^{d+1}}{v_{\text{F}}^2 T^{d+1}}, \quad (3.37)$$

and we find $A_{\text{ph-ph, coll}} \gg A_{e\text{-ph}}$ at $T > T_{\text{BG}}$, assuming that $D_{e\text{-ph}}$ and D_{ph} are similar magnitude and approximately momentum-independent. It suggests that due to the phonon-phonon interaction, the rate for $|\text{H}\rangle_{\text{ph}}$ to relax to $|\text{L}\rangle_{\text{ph}}$ is much faster than that for the $|\text{1}\rangle_{\text{ph}}$ (effectively $|\text{L}\rangle_{\text{ph}}$) to relax out due to electron-phonon interaction. In another word, the total electron and phonon momentum remains a good conserved quantity at the time scale of $\gamma_{e\text{-ph}}^{-1}$, thus the electron-phonon fluid is well-defined at $T > T_{\text{BG}}$. For concreteness, let's write the momentum as

$$|P\rangle \propto c_2 |0\rangle_e + c_1 c_2 |\text{L}\rangle_{\text{ph}} + c_1 |\text{H}\rangle_{\text{ph}}, \quad (3.38)$$

where $c_{1,2}$ are dimensionless constants. The collision integral with momentum conservation is of the form

$$\langle \Phi | W | \Phi \rangle = \gamma_{e\text{-ph}} \frac{(\Phi_{\text{L}} - c_1 \Phi_{\text{e}})^2}{1 + c_1^2} + \gamma_{\text{ph-ph, coll}} \frac{(\Phi_{\text{L}} - c_2 \Phi_{\text{H}})^2}{1 + c_2^2}. \quad (3.39)$$

In the limit of $\gamma_{e\text{-ph}} / \gamma_{\text{ph-ph, coll}} \ll (1 + c_1^2)(1 + c_2^2)$, the eigenvalues of W are given by $\{0, \gamma_{e\text{-ph}}, \gamma_{\text{ph-ph, coll}}\}$ approximately. The null eigenvalue comes from momentum conservation. Notice that we obtain a looser constraint on $\gamma_{e\text{-ph}} / \gamma_{\text{ph-ph, coll}}$ since $c_1 > 1$ at high temperature. The eigenstate, corresponding to the eigenvalue $\gamma_{\text{ph-ph}}$, is $c_1(1 + c_1^2)^{-1}(\gamma_{e\text{-ph}} / \gamma_{\text{ph-ph, coll}}) |0\rangle_e - |\text{L}\rangle_{\text{ph}} + c_2 |\text{H}\rangle_{\text{ph}}$, so that, in accordance with (3.38), electron modes are strongly suppressed in phonon-phonon collinear scattering, coinciding with the previous argument.

Observe that the modes $|\tilde{1}, m\rangle_{\text{ph}}$ (which represent the phonon momentum) are exact null vectors of the linearized phonon-phonon collision integral for $m = 0$ due to conservation of phonon energy in phonon-phonon collisions, and when $m = \pm 1$ due to conservation of momentum. Once $|m| > 1$, $|\tilde{1}, m > 1\rangle_{\text{ph}}$, will scatter non-collinearly and experience a non-collinear phonon-phonon scattering rate

$$\gamma_{\text{ph-ph, non-coll}} \sim \frac{D_{\text{ph}}}{\langle \Phi | \Phi \rangle} \left(\frac{T}{v_{\text{ph}}} \right)^{2d-1} \frac{T^2}{v_{\text{ph}}^4} \sim D_{\text{ph}} \frac{T^{d+2}}{v_{\text{ph}}^{d+3}}. \quad (3.40)$$

Formally, in the hydrodynamic calculations, the collision integral becomes

$$W' = W'_{e\text{-ph}} + (\gamma_{\text{ph-ph, non-coll}} + \gamma_{\text{ph-ph, coll}} (\mathbb{1} - \mathbb{P}_{\text{L,H}})) \sum_{|m|>1} \mathbb{P}_m \quad (3.41)$$

where $\mathbb{P}_m = |1, m\rangle_{\text{ph}} \langle 1, m|_{\text{ph}}$ is the normalized projector onto phonon modes with ‘‘angle’’ m , and $\mathbb{P}_{\text{L,H}}$ is the projection within phonon sector making phonon momentum a null vector to the collision integral.

Results of scattering rates computed in Section 3.3 and Section 3.4 are summarized in Table 2.

4. HYDRODYNAMICS

Having developed the kinetic theory of electron phonon fluid, we can study its universal properties in the hydrodynamic limit of $\partial_t \ll \min W'_{e\text{-ph}}$. Hydrodynamics is an effective theory approach and describes the late time dynamics of the conserved quantities. In our rotationally invariant electron-phonon fluid, there are charge, energy and momentum:

$$\partial_t \rho + \partial_i J_i = 0, \quad (4.1a)$$

$$\partial_t \epsilon + \partial_i J_{Ei} = 0, \quad (4.1b)$$

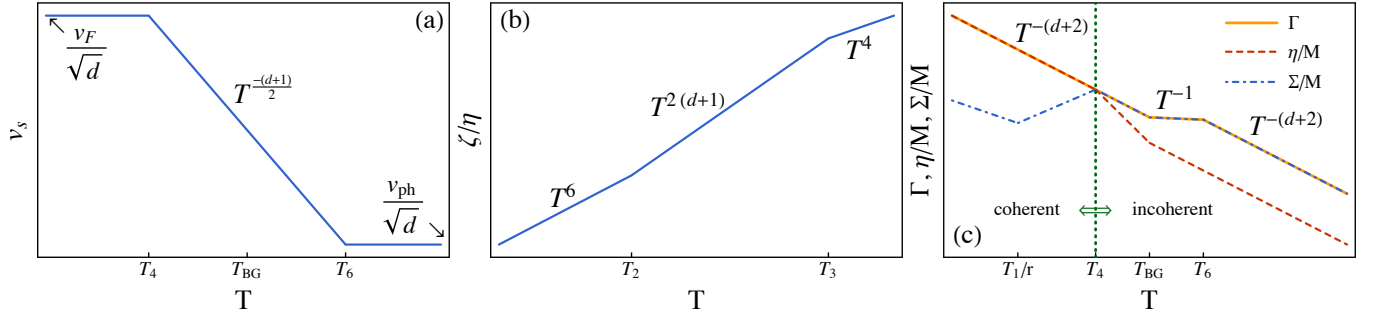


FIG. 1. Hydrodynamics of electron-phonon fluid. (a): Log-log plot of sound velocity against temperature. (b): Log-log plot of bulk viscosity over shear viscosity against temperature. (c): Log-log plot of diffusion constant (orange thick line), shear viscosity (red dashed line) and incoherent conductivity (blue dot-dashed line) against temperature. In (c), the vertical green line separates the fluid into coherent and incoherent.

$$\partial_t p_i + \partial_j \tau_{ij} = 0, \quad (4.1c)$$

and

$$\begin{aligned} \begin{pmatrix} J_i \\ J_{Ei} \end{pmatrix} &= \begin{pmatrix} \rho \\ \epsilon + P \end{pmatrix} u_i - \Sigma_0 \partial_i \begin{pmatrix} \mu \\ T \end{pmatrix} + \dots \\ \tau_{ij} &= -\eta(\partial_i u_j + \partial_j u_i - \frac{2}{d} \delta_{ij} \partial_k u_k) - \zeta \delta_{ij} \partial_k u_k + \delta_{ij} P + \dots \end{aligned} \quad (4.2)$$

where Σ_0 is the incoherent conductivity matrix [36, 49], η is the shear viscosity and ζ is the bulk viscosity. The hydrodynamic quasinormal modes, which are the degrees of freedom of the effective theory, are found by substituting a plane wave ansatz into (4.1). We obtain a sound mode

$$\omega = \pm v_s k - i \Gamma k^2 + \mathcal{O}(k^3) \quad (4.3)$$

where v_s is the sound velocity, and Γ is the sound wave's “diffusion constant”. Apart from the sound mode, the perpendicular components of the velocity field (the transverse momentum) obey a diffusion equation controlled by the shear viscosity:

$$\omega = -i \frac{\eta}{M} k^2. \quad (4.4)$$

For convenience, we introduce operators: $\rho_A = (\rho, \epsilon)$, $\mu_A = (\mu, T)$, $A = 1, 2$. Assisted with kinetic formalism, we could calculate explicitly the transport coefficients in hydrodynamic equations in following subsections.

4.1. Speed of sound

Based on (3.19c) and (3.19d), we can derive the susceptibility matrix

$$\chi \equiv \frac{\partial \rho_A}{\partial \mu_B} = \begin{pmatrix} \frac{\partial \rho}{\partial \mu} & \frac{\partial \rho}{\partial T} \\ \frac{\partial \epsilon}{\partial \mu} & \frac{\partial \epsilon}{\partial T} \end{pmatrix} \approx \begin{pmatrix} \frac{d\nu}{2} & \frac{\partial}{\partial T} (\frac{\nu}{2} \partial_p v_F a^2) \\ \frac{\partial}{\partial \mu} (\frac{\nu v_F^2 a^2}{2T}) & \nu (\frac{\pi^2}{6} + I^2 \frac{dT^{d-1}}{v_{ph}^d \nu}) \end{pmatrix} \Rightarrow \chi^{-1} \approx \begin{pmatrix} \frac{2}{d\nu} & \mathcal{O}(\frac{T}{T_F}) \\ \mathcal{O}(\frac{T}{T_F}) & \frac{d\nu}{2 \det \chi} \end{pmatrix}, \quad (4.5)$$

where

$$\det \chi \approx \frac{d}{2} \left(\frac{\pi^2}{6} \nu^2 + I^2 \frac{dT^{d-1}}{v_{ph}^d \nu} \right). \quad (4.6)$$

Note that $\det \chi$ switches from being dominated by electrons to dominated by phonons at $T \sim T_3$. Keeping the leading order in T/T_F , the sound wave velocity of the quasinormal mode is given by

$$v_s = \sqrt{\frac{\rho_A \chi_{AB}^{-1} \rho_B}{M}} \approx \sqrt{\left(\frac{1}{d} \nu^2 \mu^2 + 2d \left(\frac{\nu^2}{2} v_F^2 p_F^2 \right)^2 \frac{(\bar{a}^2 + r^2 \bar{w}^2)^2}{T^2 \det \chi} \right) / \nu^2 p_F^2 (1 + \bar{a}^2 + \bar{w}^2)}$$

$$\approx \begin{cases} \sqrt{\frac{\mu^2}{d p_F^2}} = \frac{v_F}{\sqrt{d}} & T < T_4 \\ \sqrt{\frac{\mu^2}{d p_F^2 \bar{w}^2}} = \frac{v_F}{\bar{w} \sqrt{d}} & T_4 < T < T_6 \\ \sqrt{\frac{v_F^2 r^2}{d}} = \frac{v_{\text{ph}}}{\sqrt{d}} & T_6 < T \ll T_F \end{cases} \quad (4.7)$$

where repeated indices are summed. To obtain the last phonon-limited sound velocity, we have used the identity (2.5) to replace constant I with dimensionless \bar{w} . The scaling is shown in Figure 1(a). We observe that when temperature is low enough, electron phonon fluid is more like a Fermi liquid with sound velocity given by the Fermi velocity. When the temperature rises over T_4 , the phonon momentum starts to dominate over the total momentum such that the sound velocity is corrected by a factor of $1/\bar{w} < 1$. With Fermi velocity and phonon momentum weight appearing in the same expression, this regime cannot be thought of as phonon-dominated or electron-dominated, but electrons and phonons together flow as a single unified fluid. When the temperature is higher than T_6 , the sound velocity is controlled by the phonon velocity v_{ph}/\sqrt{d} .

4.2. Shear viscosity

To calculate the shear viscosity, we first write down the momentum current (stress tensor) operator. Focusing on $d = 2$ for ease of presentation:

$$\begin{aligned} |\tau_{xx}\rangle - |\tau_{yy}\rangle &= \int d^d p p v_p \cos 2\theta |\mathbf{p}\rangle + v_{\text{ph}} \int d^d q q \cos 2\theta |\mathbf{q}\rangle \\ &= \frac{1}{2} (p_F v_F |\tilde{0}, 2\rangle_e + (v_F + p_F \partial_p v_F) |\tilde{1}, 2\rangle_e + \partial_p v_F |\tilde{2}, 2\rangle_e + \dots + v_{\text{ph}} |\tilde{1}, 2\rangle_{\text{ph}} + (m = -2)). \end{aligned} \quad (4.8)$$

In above equation, all the modes are in $m = \pm 2$ sector, thus there is no good conservation law. We then approximate that the collision integral in this sector is diagonal, and obtain

$$\begin{aligned} \eta &= (\langle \tau_{xx} | - \langle \tau_{yy} |) W'^{-1} (|\tau_{xx}\rangle - |\tau_{yy}\rangle) \\ &\approx \nu \mu^2 \gamma_e^{-1} + w^2 v_{\text{ph}}^2 (\gamma_{\text{ph}} + \gamma_{\text{ph-ph}})^{-1} \\ &\approx \begin{cases} \nu \mu^2 \gamma^{-1} & T < T_{\text{BG}} \\ \nu \mu^2 (\bar{\gamma}^{-1} + r^2 \bar{w}^2 \gamma_{\text{ph-ph}}^{-1}) & T_{\text{BG}} < T \ll T_F \end{cases} \end{aligned} \quad (4.9)$$

The change in η manifests in Bloch-Grüneisen effect with $\gamma \rightarrow \bar{\gamma}$. Note that when $T > T_{\text{BG}}$, the shear viscosity may still be dominated by the electron modes due to the fast phonon-phonon scattering (including both collinear and non-collinear scattering). However, it is also plausible that, depending on microscopic details, above $T > T_{\text{BG}}$ phonons can dominate the shear viscosity.

4.3. Bulk viscosity

Unlike the shear viscosity, to estimate the bulk viscosity, we need to search for the non-conserved part of the trace of the momentum current. Again writing formulas in $d = 2$ for illustrative purposes, we obtain

$$\begin{aligned} |\tau_{xx}\rangle + |\tau_{yy}\rangle &= \int d^d p p v_p |\mathbf{p}\rangle + v_{\text{ph}} \int d^d q q |\mathbf{q}\rangle \\ &= p_F v_F |\tilde{0}, 0\rangle_e + (v_F + p_F \partial_p v_F) |\tilde{1}, 0\rangle_e + \partial_p v_F |\tilde{2}, 0\rangle_e + \dots + v_{\text{ph}} |\tilde{1}, 0\rangle_{\text{ph}}. \end{aligned} \quad (4.10)$$

To this end, we consider the incoherent momentum current

$$\begin{aligned}
(|\tau_{xx}\rangle + |\tau_{yy}\rangle)_{\text{inc}} &\equiv |\tau_{xx}\rangle + |\tau_{yy}\rangle - \frac{\langle \tilde{\epsilon} | (|\tau_{xx}\rangle + |\tau_{yy}\rangle) | \tilde{\epsilon} \rangle}{\langle \tilde{\epsilon} | \tilde{\epsilon} \rangle} |\tilde{\epsilon}\rangle - \frac{\langle \rho | (|\tau_{xx}\rangle + |\tau_{yy}\rangle) | \rho \rangle}{\langle \rho | \rho \rangle} |\rho\rangle \\
&\approx \frac{2r^2\bar{w}^2}{\langle \tilde{\epsilon} | \tilde{\epsilon} \rangle} v_{\text{F}} |\tilde{1}, 0\rangle_{\text{e}} - \frac{a^2}{\langle \tilde{\epsilon} | \tilde{\epsilon} \rangle} v_{\text{ph}} |\tilde{1}, 0\rangle_{\text{ph}} + \dots + |\tilde{2}, 0\rangle_{\text{e}}.
\end{aligned} \tag{4.11}$$

While vanishing for a quadratic electron band, the $|\tilde{2}, 0\rangle_{\text{e}}$ contribution above is present for a generic dispersion relation. In above, we omit the temperature-independent (also v_{ph} -independent) prefactor to simplify the scaling analysis. The bulk viscosity is given by

$$\begin{aligned}
\zeta &= (\langle \tau_{xx} | + \langle \tau_{yy} |)_{\text{inc}} W'_{\text{e-ph}}{}^{-1} (|\tau_{xx}\rangle + |\tau_{yy}\rangle)_{\text{inc}} \\
&= \nu (v_{\text{F}} p_{\text{F}})^2 \left(\frac{r^4 \bar{a}^2 \bar{w}^4 \gamma_{\text{e}}'^{-1} + r^2 \bar{a}^4 \bar{w}^2 \gamma_{\text{ph}}'^{-1} - 2r^3 \bar{a}^3 \bar{w}^3 \gamma_{\text{e-ph}}'^{-1}}{(\bar{a}^2 + r^2 \bar{w}^2)^2} + \left(\frac{T}{T_{\text{F}}} \right)^4 \gamma_{\text{e}}''^{-1} \right),
\end{aligned} \tag{4.12}$$

where $\gamma_{\text{e}}'' = \langle 2 | W_{\text{e-ph}} | 2 \rangle_{\text{e}} \approx r^4 \bar{a}^{-2} \gamma$ when $T < T_{\text{BG}}$ (see Appendix B). After some algebra, we find that

$$\zeta \approx \begin{cases} \nu (v_{\text{F}} p_{\text{F}})^2 \gamma^{-1} r^{-4} \bar{a}^6 \sim \eta r^{-4} (T/T_{\text{F}})^6 & T < T_2 \\ \nu (v_{\text{F}} p_{\text{F}})^2 \gamma^{-1} r^2 \bar{w}^4 \sim \eta r^{-(2d+2)} (T/T_{\text{F}})^{2d+2} & T_2 < T < T_3 \\ \nu (v_{\text{F}} p_{\text{F}})^2 \gamma^{-1} r^{-2} \bar{a}^4 \sim \eta r^{-2} (T/T_{\text{F}})^4 & T_3 < T < T_{\text{BG}} \\ \nu (v_{\text{F}} p_{\text{F}})^2 \bar{\gamma}^{-1} r^{-2} \bar{a}^4 \sim \eta r^{-2} (T/T_{\text{F}})^4 & T_{\text{BG}} < T \ll T_{\text{F}} \end{cases}. \tag{4.13}$$

The first two critical temperatures are unique to the bulk viscosity (see Figure 1(b)). T_2 is the critical temperature below which the incoherent momentum current, i.e. the non-conserved part of the momentum current, is predominated by $|\tilde{2}, 0\rangle_{\text{e}}$. This is the regime where electron-phonon fluid is completely dominated by the electron modes. However, unlike a generic Fermi liquid, the relation $\zeta/\eta \sim (T/T_{\text{F}})^4$ is not satisfied in such electron-phonon fluid even $T < T_2$ because $\gamma_{\text{e}}'' \neq \gamma_{\text{e}}$ for electron-phonon interaction. After all, the radial deformations of the Fermi surface decay quite differently from radially uniform deformations. The electron-phonon fluid is intrinsically different from the Fermi liquid dominated by electron-electron interactions, even if transport is dominated by the electron modes. T_3 is the critical temperature above which the phonon energy starts to dominate the total energy.

Note that the bulk viscosity is much smaller than the shear viscosity at low temperatures. Interestingly, since shear viscosity is suppressed at high temperature due to the non-collinear phonon-phonon scattering, in principle the bulk viscosity can exceed the shear viscosity at sufficiently high temperature. The non-vanishing of bulk viscosity at high temperatures also implies that the relativistic electron-phonon fluid at high temperature is strongly non-conformal, as conformal symmetry fixes $\zeta = 0$ [37]. Note that a phonon fluid on its own, however, would have $\zeta = 0$ since $(|\tau_{xx}\rangle + |\tau_{yy}\rangle)_{\text{inc}} = 0$, as can readily be seen from (4.11).⁴

4.4. Incoherent conductivities

To calculate the incoherent conductivities, we need first to compute the incoherent currents. The incoherent charge current is given by

$$\begin{aligned}
\| |J_{\text{inc}}\rangle \| &\equiv \left\| |J_x\rangle - \frac{\langle p_x | J_x \rangle}{\langle p_x | p_x \rangle} |p_x\rangle \right\| \approx \sqrt{\frac{e^2 \nu}{2}} \sqrt{(v_{\text{F}}^2 + p_{\text{F}}^2 \partial_p v_{\text{F}}^2 \bar{a}^2) - \frac{(v_{\text{F}} + p_{\text{F}} \partial_p v_{\text{F}} \bar{a}^2)^2}{1 + \bar{a}^2 + \bar{w}^2}} \\
&\approx \begin{cases} \sqrt{\nu/2} e |p_{\text{F}} \partial_p v_{\text{F}} - v_{\text{F}} \bar{a}| \bar{a} \sim T/T_{\text{F}} & T < T_1 \\ \sqrt{\nu/2} e v_{\text{F}} \bar{w} \sim r^{-(d+2)/2} (T/T_{\text{F}})^{(d+1)/2} & T_1 < T < T_4 \\ \sqrt{\nu/2} e v_{\text{F}} \sim T^0 & T_4 < T \ll T_{\text{F}} \end{cases}.
\end{aligned} \tag{4.14}$$

As $\| |J_x\rangle \| \approx \sqrt{\nu/2} e v_{\text{F}} \sim T^0$, we find that when $T < T_4$ the charge current is coherent; when $T > T_4$ the charge current is incoherent. To understand this, we note that T_4 is the temperature above which the phonon momentum starts to dominate the total momentum, however, the charge is fully carried by the electron momentum, and such mismatch in

⁴ This remains true until we consider subleading p^2 corrections to the acoustic phonon dispersion relation (3.14).

charge current and momentum operator results in an incoherent current. Note that when charge current is coherent, the incoherent current has different scalings from $|J_{\text{inc}}\rangle \sim \bar{a}$ to $|J_{\text{inc}}\rangle \sim \bar{w}$ signaled by the critical temperature T_1 . This comes from the competition between relative weights of total momentum in Fermi surface fluctuation and phonon momentum.

Next, the incoherent heat current is given by

$$\begin{aligned} \||Q_{\text{inc}}\rangle\| &\equiv \left\| |Q_x\rangle - \frac{\langle p_x | Q_x \rangle}{\langle p_x | p_x \rangle} |p_x\rangle \right\| \approx \sqrt{\frac{\nu}{2} p_{\text{F}}^2 v_{\text{F}}^4} \sqrt{(\bar{a}^2 + r^4 \bar{w}^2) - \frac{(\bar{a}^2 + r^2 \bar{w}^2)^2}{1 + \bar{w}^2}} \\ &\approx \sqrt{\frac{\nu}{2} p_{\text{F}}^2 v_{\text{F}}^4 \bar{a}^2} \sim T/T_{\text{F}}, \quad T \ll T_{\text{F}}. \end{aligned} \quad (4.15)$$

Since

$$\||Q_x\rangle\| = \sqrt{\frac{\nu}{2} p_{\text{F}}^2 v_{\text{F}}^4 (\bar{a}^2 + r^4 \bar{w}^2)} \approx \begin{cases} \sqrt{\frac{\nu}{2} p_{\text{F}}^2 v_{\text{F}}^4 \bar{a}^2} \sim T/T_{\text{F}} & T < T_7 \\ \sqrt{\frac{\nu}{2} p_{\text{F}}^2 v_{\text{F}}^4 \bar{w}^2} \sim r^{-(d-2)/2} (T/T_{\text{F}})^{(d+1)/2} & T_7 < T \ll T_{\text{F}} \end{cases}, \quad (4.16)$$

we find that when $T \ll T_7$ the heat current is incoherent; when $T \gg T_7$ the heat current is coherent. In contrast, the energy current

$$|J_{\text{Ex}}\rangle = \frac{\mu}{e} |J_x\rangle + |Q_x\rangle. \quad (4.17)$$

is dominated by the charge current when $T \ll T_4$ (and is thus trivially coherent); moreover, $|J_{\text{Ex}}\rangle \approx \mu |J_x\rangle$ has the same coherent-incoherent transition at $T \sim T_4$. When $T \gg T_8$, however, $|J_{\text{Ex}}\rangle \approx |Q_x\rangle$. Because when $T \gg T_8$, the sound velocity $v_s \approx v_{\text{ph}}/\sqrt{d}$ arises from a thermodynamic equation of state which is dominated by the phonons, and there is a small incoherent thermal conductivity, we claim that the fluid behaves as a nearly charge-neutral, approximately relativistic [50] fluid.

Within the framework of kinetic theory formalism, the incoherent conductivity matrix Σ_0 can be written as

$$\Sigma_{AB} = \begin{pmatrix} \sigma_{\text{inc}} & T\alpha_{\text{inc}} \\ T\alpha_{\text{inc}} & T\bar{\kappa}_{\text{inc}} \end{pmatrix} = \begin{pmatrix} \langle J_{\text{inc}} | \\ \langle Q_{\text{inc}} | \end{pmatrix} W_{\text{e-ph}}'^{-1} \begin{pmatrix} |J_{\text{inc}}\rangle \\ |Q_{\text{inc}}\rangle \end{pmatrix}, \quad (4.18)$$

where all the quantities point to x direction. Explicit expressions and scalings of each element are:

$$\begin{aligned} \sigma_{\text{inc}} &\approx \frac{e^2 v_{\text{F}}^2 \nu}{(1 + \bar{a}^2 + \bar{w}^2)^2} \left\{ [(1 - p_{\text{F}} \partial_p \ln v_{\text{F}}) \bar{a}^2 + \bar{w}^2]^2 \gamma_e^{-1} + [1 - (1 + \bar{w}^2) p_{\text{F}} \partial_p \ln v_{\text{F}}]^2 \bar{a}^2 \gamma_e'^{-1} + \bar{w}^2 \gamma_{\text{ph}}^{-1} \right\} \\ &\approx \begin{cases} e^2 (v_{\text{F}} - p_{\text{F}} \partial_p v_{\text{F}})^2 \nu \gamma^{-1} r^{-2} \bar{a}^4 \sim r^{-2} (T/T_{\text{F}})^{-(d-2)} & T < T_1/r \\ 2e^2 v_{\text{F}}^2 \nu \gamma^{-1} \bar{w}^4 \sim r^{-2(d+2)} (T/T_{\text{F}})^d & T_1/r < T < T_4 \\ 2e^2 v_{\text{F}}^2 \nu \gamma^{-1} \sim (T/T_{\text{F}})^{-(d+2)} & T_4 < T < T_{\text{BG}} \\ 2e^2 v_{\text{F}}^2 \nu \bar{\gamma}^{-1} \sim (T/T_{\text{F}})^{-1} & T_{\text{BG}} < T \ll T_{\text{F}} \end{cases}, \end{aligned} \quad (4.19a)$$

$$\begin{aligned} T\bar{\kappa}_{\text{inc}} &\approx \frac{\nu p_{\text{F}}^2 v_{\text{F}}^4}{(1 + \bar{a}^2 + \bar{w}^2)^2} \left\{ (\bar{a}^2 + r^2 \bar{w}^2)^2 \gamma_e^{-1} + (1 + \bar{w}^2)^2 \bar{a}^2 \gamma_e'^{-1} + (r^2 - \bar{a}^2)^2 \bar{w}^2 \gamma_{\text{ph}}^{-1} \right\} \\ &\approx \begin{cases} \nu v_{\text{F}}^4 p_{\text{F}}^2 \gamma^{-1} \frac{\bar{a}^4}{r^2} \sim r^{-2} (T/T_{\text{F}})^{-(d-2)} & T < T_{\text{BG}} \\ \nu v_{\text{F}}^4 p_{\text{F}}^2 \gamma^{-1} \bar{a}^2 \sim T/T_{\text{F}} & T_{\text{BG}} < T \ll T_{\text{F}} \end{cases}, \end{aligned} \quad (4.19b)$$

$$\begin{aligned} T\alpha_{\text{inc}} &\approx -\frac{e\nu v_{\text{F}}^3 p_{\text{F}}}{(1 + \bar{a}^2 + \bar{w}^2)^2} \left\{ [(1 - p_{\text{F}} \partial_p \ln v_{\text{F}}) \bar{a}^2 + \bar{w}^2] (\bar{a}^2 + r^2 \bar{w}^2) \gamma_e^{-1} \right. \\ &\quad \left. + [1 - (1 + \bar{w}^2) p_{\text{F}} \partial_p \ln v_{\text{F}}] (1 + \bar{w}^2) \bar{a}^2 \gamma_e'^{-1} + (r^2 - \bar{a}^2) \bar{w}^2 \gamma_{\text{ph}}^{-1} \right\} \\ &\approx \begin{cases} -e\nu v_{\text{F}}^2 p_{\text{F}} (v_{\text{F}} - p_{\text{F}} \partial_p v_{\text{F}}) \gamma^{-1} r^{-2} \bar{a}^4 \sim r^{-2} (T/T_{\text{F}})^{-(d-2)} & T < T_3 \\ -2e\nu v_{\text{F}}^3 p_{\text{F}} \gamma^{-1} r^2 \bar{w}^4 \sim r^{-2(d+1)} (T/T_{\text{F}})^d & T_3 < T < T_4 \\ -2e\nu v_{\text{F}}^3 p_{\text{F}} \gamma^{-1} r^2 \sim r^2 (T/T_{\text{F}})^{-(d+2)} & T_4 < T < T_{\text{BG}} \\ e\nu v_{\text{F}}^3 p_{\text{F}} \bar{\gamma}^{-1} \bar{a}^2 \sim T/T_{\text{F}} & T_{\text{BG}} < T \ll T_{\text{F}} \end{cases}. \end{aligned} \quad (4.19c)$$

We observe that one might naively expect that for a Galilean dispersion relation in which $v_F - p_F \partial_p v_F = 0$, that both σ_{inc} and α_{inc} must vanish identically since there is no incoherent current: electrical current and momentum are proportional [36]. However, this is not true, because the presence of phonons dispersion relation necessarily leads to breaking of Galilean invariance.

Now we are ready to compute the diffusion constant

$$\Gamma = \frac{2^{\frac{d-1}{d}} \eta + \zeta}{M} + \frac{\Sigma}{M}, \quad (4.20)$$

where

$$\Sigma \equiv \frac{\rho_A \chi_{AC}^{-1} \Sigma_{CD} \chi_{DB}^{-1} \rho_B}{v_s^2} \quad (4.21)$$

is a contribution to the decay rate arising from incoherent conductivities. After some algebra, we find that

$$\Gamma \sim \begin{cases} \gamma^{-1} \sim (T/T_F)^{-(d+2)} & T < T_{\text{BG}} \\ \tilde{\gamma}^{-1} \sim (T/T_F)^{-1} & T_{\text{BG}} < T < T_6 \\ \tilde{\gamma}^{-1} r^{-2} \tilde{w}^{-2} \sim r^d (T/T_F)^{-(d+2)} & T_6 < T \ll T_F \end{cases} \quad (4.22)$$

The scaling is shown in Figure 1(c). When $T < T_4$, the shear viscosity, given by the electron modes, controls the diffusion of the fluid, i.e. $\eta > \Sigma$. When $T > T_4$, the diffusion constant starts to be dominated by the incoherent conductivity, i.e. $\eta < \Sigma$, but the scaling do not change. The interplay between shear viscosity and incoherent conductivity implies a transition from coherent to incoherent, giving rise to a breakdown of Galilean invariance.

4.5. Plasmons

Although short-range interactions between individual electrons are assumed to be negligible in our model (for pedagogical purposes), the long-range Coulomb interaction, responsible for the density-density interaction gives rise to qualitative changes in the hydrodynamic dispersion relations, and so we will briefly address what happens in the presence of unscreened and long-range Coulomb interactions. We account for the long-range Coulomb interaction by replacing the chemical potential with the external electrochemical potential [39, 51, 52]

$$\partial_i \mu \rightarrow \partial_i \mu - F_{\text{ext}} \quad (4.23)$$

where

$$F_{\text{ext}} = -\partial_i \int d^d y \frac{e^2}{|x-y|} (\rho(y) - \rho_0). \quad (4.24)$$

Fourier transforming (4.2), we obtain the frequency-momentum space hydrodynamic equation

$$-i\omega \chi_{AB} \delta \mu_B + ik \rho_A \delta u_i + k^2 \tilde{\Sigma}_{AB} \delta \mu_B = 0 \quad (4.25a)$$

$$-i\omega M \delta u_i + ik \tilde{\rho}_A \delta \mu_A + \left(\eta + \frac{2d-2}{d} \zeta \right) k^2 \delta u_i = 0 \quad (4.25b)$$

where we assume \mathbf{k} is parallel to $\delta \mathbf{u}$ and

$$\tilde{\rho}_1 = (1 + U(k)\nu)\rho_1, \quad \tilde{\rho}_2 = \rho_2, \quad \tilde{\Sigma}_{A1} = (1 + U(k)\nu)\Sigma_{A1}, \quad \tilde{\Sigma}_{A2} = \Sigma_{A2}, \quad (4.26)$$

with $F_{\text{ext}}(k) = -ikU(k)\nu\delta\mu$. Note that for tilded operators, only components related to the chemical potential are corrected by the long-range Coulomb interaction. We take $d = 2$ for illustration. For small wave vector, we can approximate

$$(1 + U(k)\nu)k^2 \approx 2\pi e^2 \nu |k|. \quad (4.27)$$

Solving (4.25), we have the dispersion relation of plasmons

$$\omega_{\text{plasmon}} = \pm \sqrt{\frac{\tilde{\rho}_{AX} \chi_{AB}^{-1} \rho_B}{M} k^2 - i \left(\frac{2(d-1)\eta}{dM} + \frac{\tilde{\rho}_{AX} \chi_{AC}^{-1} \tilde{\Sigma}_{CD} \chi_{DB}^{-1} \rho_B}{\tilde{\rho}_{AX} \chi_{AB}^{-1} \rho_B} \right) k^2} \approx \begin{cases} \pm \frac{v_F}{\sqrt{d}} \sqrt{2\pi e^2 \nu |k|} - i\nu \mu^2 \gamma^{-1} (k^2 + \bar{a}^4 (2\pi e^2 \nu) |k|) & T < T_1 \\ \pm \frac{v_F}{\sqrt{d}} \sqrt{2\pi e^2 \nu |k|} - i\nu \mu^2 \gamma^{-1} (k^2 + \bar{w}^4 (2\pi e^2 \nu) |k|) & T_1 < T < T_4 \\ \pm \frac{v_F}{\bar{w} \sqrt{d}} \sqrt{2\pi e^2 \nu |k|} - i\nu \mu^2 \gamma^{-1} (k^2 / \bar{w}^2 + (2\pi e^2 \nu) |k|) & T_4 < T < T_{\text{BG}} \\ \pm \frac{v_F}{\bar{w} \sqrt{d}} \sqrt{2\pi e^2 \nu |k|} - i\nu \mu^2 \bar{\gamma}^{-1} (k^2 / \bar{w}^2 + (2\pi e^2 \nu) |k|) & T_{\text{BG}} < T < T_6 \\ \pm \frac{v_F}{\bar{w} \sqrt{d}} \sqrt{2\pi e^2 \nu |k| + r^2 \bar{w}^2 k^2} - \frac{i\nu \mu^2 \bar{a}^4 k^2 + (2\pi e^2 \nu)^2}{\bar{\gamma} 2\pi e^2 \nu + r^2 \bar{w}^2 |k|} |k| & T_6 < T \ll T_F \end{cases} \quad (4.28)$$

In this expression we have used the fact that $\eta \gg \zeta$ to simplify the result.

For $T < T_6$, $\omega_{\text{plasmon}} \sim \sqrt{k}$ manifests the conventional plasmon dispersion relation [53–55]

$$\omega_{\text{plasmon}} = \sqrt{\frac{2\pi e^2 n}{m} |k|} + \dots; \quad (4.29)$$

note we have used the identity (2.1). Importantly, however, the prefactor of $|k|$ is also affected by the large contribution of phonons to M (and therefore the effective value of m) above $T > T_4$, and so it will exhibit the same dramatic T -dependence as the sound velocity (4.7). This provides a clear difference with the usual electron fluid where electron-electron interactions dominate [39, 56]. When the temperature is below T_4 , the hydrodynamic is coherent, and the imaginary part, known as the plasmon decay, is the usual sound wave decay (4.20), but with a crossover to the more severe plasmon decay $\delta\omega_{\text{plasmon}} \sim -i\gamma^{-1}|k|$ at ultra low k . However, when $T > T_4$, this plasmon decay starts to dominate indicating the increasingly incoherent nature of the charge current.

As the temperature keeps increasing, the plasmon mode starts to transform into the phonon-limited sound mode $\omega \sim v_{\text{ph}}/\sqrt{d}$ when $T > T_6$, at short enough distance scales. The long distance physics with small enough k ($r^2 \bar{w}^2 |k| < 2\pi e^2 \nu$) is always controlled by the long-range Coulomb interactions. Interestingly, the plasmon decay in the high temperature regime shows a dramatically different behavior. In the regime $T_6 < T \ll T_F$, the second term \bar{a}^4 in imaginary part could be neglected resulting in a k -independent plasmon decay in $d = 2$ at short distance. Similar behavior exists in hydrodynamics with momentum relaxed by impurities [36], where such k -independent decay is given by $-i\tau_{\text{imp}}^{-1}$. However, here, it is induced purely through the long-range Coulomb interaction. Notice that such k -independent plasmon decay will crossover to the incoherent plasmon decay $\sim -i|k|$ at long distance (same as the crossover in the real part), while crossover to the sound wave decay $\sim -ik^2$ at short distance ($\bar{a}^2 |k| > 2\pi e^2 \nu$). The behaviors are summarized in Figure 2.

We emphasize that the imaginary part of the plasmon dispersion relation is also affected by impurities, recombination processes, etc., beyond our kinetic theory treatment. So it may be much easier to look for the unconventional real dispersion relation modification that we predict above in a near-term experiment.

5. THERMOELECTRIC TRANSPORT

In this section, we carefully address the interplay of both the electron- and phonon-impurity scattering and the electron-phonon scattering, but neglect the electron-electron scattering, as we have previously. We remind the readers the vector without tilde is the orthonormal basis after Gram-Schmidt method (see (3.16)), and obtain

$$\langle 0|W_{\text{imp}}^e|0\rangle_e = \Gamma_e, \quad (5.1a)$$

$$\langle 1|W_{\text{imp}}^e|1\rangle_e = \Gamma_e, \quad (5.1b)$$

$$\langle 0|W_{\text{imp}}^e|1\rangle_e = \frac{\pi T}{\sqrt{3}} \left(\frac{\partial \Gamma_e}{\partial \mu} - \frac{\partial_p v_F}{v_F^2} \Gamma_e \right) \equiv b, \quad (5.1c)$$

$$\langle 1|W_{\text{imp}}^{\text{ph}}|1\rangle_{\text{ph}} = \Gamma_{\text{ph}}, \quad (5.1d)$$

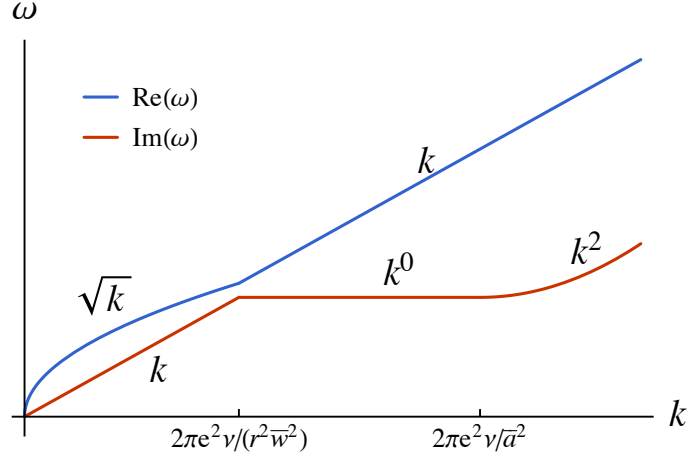


FIG. 2. Plasmon dispersion relation for electron-phonon fluid in the regime $T_6 < T \ll T_F$.

where $\Gamma_{e,\text{ph}}$ is the impurity scattering rate based upon relaxation time approximation. We work in a simple limit

$$\Gamma_{e,\text{ph}} \ll \gamma_0, \quad (5.2)$$

according to (3.26), such that the electron-phonon scattering rate could be greater than the impurity scattering rate at an appropriately temperature. Recalling (3.28), the total collision integral is given by

$$W = W_{\text{imp}}^e + W_{\text{imp}}^{\text{ph}} + W'_{e-\text{ph}}, \quad (5.3)$$

where $W'_{e-\text{ph}}$ denotes the momentum-conserving collision integral studied before. The thermoelectric conductivity matrix can be written as [41]

$$\begin{pmatrix} \sigma_{xx} & T\alpha_{xx} \\ T\alpha_{xx} & T\bar{\kappa}_{xx} \end{pmatrix} = \begin{pmatrix} \langle J_x | \\ \langle Q_x | \end{pmatrix} W^{-1} \begin{pmatrix} |J_x\rangle & |Q_x\rangle \end{pmatrix}. \quad (5.4)$$

The detailed expression can be found in Appendix C. Focusing on $T < T_{\text{BG}}$ for simplicity, we observe that

$$\sigma_{xx} = e^2 \frac{\nu}{2} v_F^2 \frac{\Gamma_{\text{ph}} + \gamma/\bar{w}^2}{\Gamma_e(\Gamma_{\text{ph}} + \gamma/\bar{w}^2) + \Gamma_{\text{ph}}\gamma} + \mathcal{O}(T^2), \quad (5.5a)$$

$$T\bar{\kappa}_{xx} = \frac{\nu}{2} p_F^2 v_F^4 \left(\frac{\bar{a}^2}{\Gamma_e + \gamma r^2/\bar{a}^2} + \frac{r^4 \bar{w}^2 (\Gamma_e + \gamma)}{\Gamma_e(\Gamma_{\text{ph}} + \gamma/\bar{w}^2) + \Gamma_{\text{ph}}\gamma} + 2r^2 \bar{a} \frac{-(b - \gamma r^2/\bar{a})\gamma + (\Gamma_e + \gamma)\gamma r^2/\bar{a}}{(\Gamma_e + \gamma r^2/\bar{a}^2)[\Gamma_e(\Gamma_{\text{ph}} + \gamma/\bar{w}^2) + \Gamma_{\text{ph}}\gamma]} \right), \quad (5.5b)$$

$$T\alpha_{xx} = -e \frac{\nu}{2} p_F^2 v_F^2 \left(\frac{r^2 \gamma}{\Gamma_e(\Gamma_{\text{ph}} + \gamma/\bar{w}^2) + \Gamma_{\text{ph}}\gamma} + \frac{\bar{a}^2}{\Gamma_e + \gamma r^2/\bar{a}^2} + \bar{a} \frac{-(\Gamma_{\text{ph}} + \gamma/\bar{w}^2)(b - \gamma r^2/\bar{a}) + \gamma^2 r^2/(\bar{a}\bar{w}^2)}{(\Gamma_e + \gamma r^2/\bar{a}^2)[\Gamma_e(\Gamma_{\text{ph}} + \gamma/\bar{w}^2) + \Gamma_{\text{ph}}\gamma]} \right). \quad (5.5c)$$

Several remarks follow the above equations. First, unlike the electron-electron interaction [41], the electrical conductivity can be more strongly affected by the electron-phonon interaction if Γ_{ph} is not negligible. More drastic is the correction to thermal conductivity, as well as thermoelectric conductivity. Second, all the thermodynamic properties have a divergence in the limit $\Gamma_{e,\text{ph}} \rightarrow 0$. This is a universal result for any hydrodynamic fluid with translation symmetry [36]. However, for the experimental thermal conductivity

$$T\kappa_{xx} = T\bar{\kappa}_{xx} - \frac{(T\alpha_{xx})^2}{\sigma_{xx}} \approx \frac{\nu}{2} p_F^2 v_F^4 \left(\frac{\bar{a}^2}{\Gamma_e + \gamma r^2/\bar{a}^2} + \frac{r^4 \bar{w}^2}{\Gamma_{\text{ph}} + \gamma/\bar{w}^2} \right), \quad (5.6)$$

such divergence disappears consistently. Consequently, the ratio of the experimental thermal and electrical conductivity, i.e. the Lorenz number L , approaches zero in the (hydrodynamic) limit $\Gamma_{e,\text{ph}} \rightarrow 0$. In particular, a controlled way to estimate how clean a material should be to have a divergent Lorenz number is to compare the non-diverging and diverging term inside the thermal conductivity (5.5b). By assuming $\Gamma_{\text{ph}} = 0$ in the first place, we find that as long as

$$\Gamma_e \lesssim \frac{\gamma r^4 \bar{w}^2}{\bar{a}^2}, \quad T < T_{\text{BG}} \quad (5.7)$$

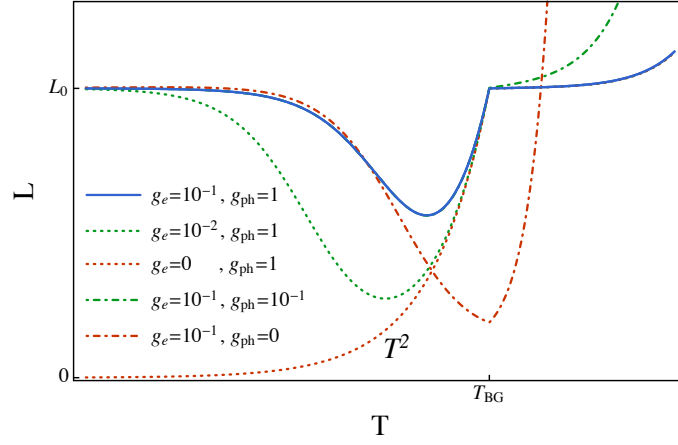


FIG. 3. Lorenz number versus temperature with five different impurity scattering rates. The kink at T_{BG} comes from the fact that the electron-phonon scattering rate in our model has a jump there.

the Lorenz number $L \ll L_0$, where $L_0 = \pi^2/3e^2$ is the non-interacting Lorenz number, and can become arbitrarily small. This effect is well understood [36]: as $\Gamma_e \rightarrow 0$, at any finite charge density σ_{xx} is divergent while κ_{xx} remains finite. Another feature that our model hold is that in the non-interacting limit $\gamma \rightarrow 0$, which corresponds to $T \rightarrow 0$, both the WF law and Mott law are simultaneously recovered so long as the impurity scattering rate is not zero, as in a normal metal [41].

After some algebra, we determine the Lorenz number with finite impurity scattering:

$$L \equiv \frac{\kappa_{xx}}{T\sigma_{xx}} \approx \begin{cases} L_0 \left(\frac{\Gamma_e(\Gamma_{\text{ph}} + \gamma/\bar{w}^2) + \Gamma_{\text{ph}}\gamma}{(\Gamma_e + \gamma r^2/\bar{a}^2)(\Gamma_{\text{ph}} + \gamma/\bar{w}^2)} + \frac{r^4\bar{w}^2}{\bar{a}^2} \frac{\Gamma_e(\Gamma_{\text{ph}} + \gamma/\bar{w}^2) + \Gamma_{\text{ph}}\gamma}{(\Gamma_{\text{ph}} + \gamma/\bar{w}^2)^2} \right) & T < T_{\text{BG}} \\ L_0 \left(\frac{\Gamma_e(\Gamma_{\text{ph}} + \bar{\gamma}/\bar{w}^2) + \Gamma_{\text{ph}}\bar{\gamma}}{(\Gamma_e + \bar{\gamma})(\Gamma_{\text{ph}} + \bar{\gamma}/\bar{w}^2)} + \frac{r^4\bar{w}^2}{\bar{a}^2} \frac{\Gamma_e(\Gamma_{\text{ph}} + \bar{\gamma}/\bar{w}^2) + \Gamma_{\text{ph}}\bar{\gamma}}{(\Gamma_{\text{ph}} + \bar{\gamma}/\bar{w}^2)^2} \right) & T_{\text{BG}} < T \ll T_{\text{F}} \end{cases}. \quad (5.8)$$

We define the ratio between impurity scattering and electron-phonon scattering as

$$g_e = \frac{\Gamma_e}{r\gamma_0}, \quad (5.9a)$$

$$g_{\text{ph}} = \frac{\Gamma_{\text{ph}}}{r\gamma_0}, \quad (5.9b)$$

and we plot the Lorenz number in Figure 3 with varying $g_{e,\text{ph}}$. We find that lowering electron-impurity scattering rate Γ_e will make L/L_0 decrease at $T < T_{\text{BG}}$. We can identify the temperature where L starts to deviate from L_0 as

$$T^* \approx r g_e^{1/d} T_{\text{F}}. \quad (5.10)$$

Meanwhile, the minimum value of L is located at $T_{\text{min}} = x T_{\text{BG}}$ where x is the solution of

$$-dg_e + (d+2)g_e x^2 + 2x^{d+2} = 0. \quad (5.11)$$

Both T^* and T_{min} are impurity-dependent resulting in non-universal behaviors. The above is valid for $\Gamma_e \neq 0$, however, when we set $\Gamma_e = 0$, (5.8) reduces to $L \approx L_0 \bar{a}^2/r^2$ at low temperature indicating that L decreases at a rate of $\sim T^2$ to zero. Lowering the phonon-impurity scattering rate hardly affects L below T_{BG} , but makes L/L_0 increase more rapidly when $T > T_{\text{BG}}$. In particular $L \approx L_0$ at $T > T_{\text{BG}}$ is valid only for large enough $g_{\text{ph}} \gtrsim 1$; at high enough temperature, L will eventually surpass L_0 due to the plethora of phonon excitations at high T . However, echoing to the argument for Γ_e , the above statement about not affecting L below T_{BG} breaks down for the strict limit $\Gamma_{\text{ph}} = 0$: L would not show a rise to L_0 nearly below T_{BG} due to the fact that $L \approx L_0 \Gamma_e/(\Gamma_e + \gamma r^2/\bar{a}^2)$ and the factor must be smaller than 1 at T_{BG} . Lastly, we briefly note that our results to those in [38], which found the same qualitative physics. However, this work focuses largely on electron-phonon umklapp scattering processes, and hence their results do not see as sharp of deviations in L/L_0 . Moreover, in [38], at very high T they argue that L/L_0 decreases due to thermal smearing of the Fermi surface. This effect lies at temperatures higher than studied in this paper; however, without electron-phonon umklapp scattering, L/L_0 will eventually exceed 1.

6. MAGNETIC FIELDS

In this section, we describe the hydrodynamic coefficients upon turning on a relatively small, classical background magnetic field. For simplicity, we restrict the discussion to two-dimensional fluids, applying a magnetic field perpendicular to the plane. The Boltzmann equation reads

$$\partial_t|\Phi\rangle + \mathbf{F}_{\text{mag}} \cdot \nabla_{\mathbf{p}}|\Phi\rangle + W|\Phi\rangle = E_i|J_i\rangle, \quad (6.1)$$

where \mathbf{F}_{mag} is the Lorentz force acting merely on the electron modes:

$$(F_{\text{mag}})_i = -eB\epsilon_{ij}v_j(p). \quad (6.2)$$

We introduce the cyclotron frequency

$$\omega_c = \frac{eBv_F}{p_F}. \quad (6.3)$$

We define the collision integral $W_{\text{mag}}|\Phi\rangle = \mathbf{F}_{\text{mag}} \cdot \nabla_{\mathbf{p}}|\Phi\rangle$, and note that $\langle\Phi_1|W_{\text{mag}}|\Phi_2\rangle = -\langle\Phi_2|W_{\text{mag}}|\Phi_1\rangle$. Such antisymmetry of W_{mag} implies that these effects are, in some sense, dissipationless – however, dissipative transport coefficients can and do become dependent on B .

6.1. Viscosity

Since the magnetic field necessarily breaks momentum conservation, we must actually consider a “quasihydrodynamic” [57] limit where the magnetic field is small: $\gamma^{-1} \ll \omega_c^{-1}$ such that the momentum is still a long-lived and approximately conserved quantity. The “angle” dependence of W_{mag} on a random Ansatz follows

$$\langle 0, m' | W_{\text{mag}} | 0, m \rangle_e = \int_0^{2\pi} \frac{d\theta}{2\pi} e^{-im'\theta} (-eB\epsilon_{ij}v_j \frac{\partial}{\partial p_i}) e^{im\theta} = im\omega_c \delta_{m,m'}. \quad (6.4)$$

The shear viscosity (4.9) is modified by the magnetic field through

$$\begin{aligned} \eta &\approx \frac{\nu\mu^2}{2} \left(\frac{1}{\gamma_e + 2i\omega_c} + \frac{1}{\gamma_e - 2i\omega_c} \right) + w^2 v_{\text{ph}}^2 (\gamma_{\text{ph}} + \gamma_{\text{ph-ph}})^{-1} \\ &\approx \begin{cases} \nu\mu^2 \left(\frac{\gamma^{-1}}{1 + (2\omega_c\gamma^{-1})^2} + r^2 \bar{w}^2 (\gamma_{\text{ph}} + \gamma_{\text{ph-ph}})^{-1} \right) & T < T_{\text{BG}} \\ \nu\mu^2 \left(\frac{\bar{\gamma}^{-1}}{1 + (2\omega_c\bar{\gamma}^{-1})^2} + r^2 \bar{w}^2 (\gamma_{\text{ph}} + \gamma_{\text{ph-ph}})^{-1} \right) & T_{\text{BG}} < T \ll T_{\text{F}} \end{cases}. \end{aligned} \quad (6.5)$$

However, if the phonon-phonon scattering is weak in the sense of $D_{\text{ph}} \ll D_{\text{e-ph}}$, then the second term in the above equation could contribute non-trivially, making the electron-phonon fluid under background magnetic field an exotic fluid with unconventional shear viscosity. This is analogous, in many ways, to the emergence of incoherent conductivities spoiling the conventional Kohn’s theorem [50]. The Hall viscosity is given by

$$\begin{aligned} \eta_{\text{H}} &= (\langle \tau_{xx} | - \langle \tau_{yy} |) \gamma_{ii}^{-1} (| \tau_{xy} \rangle + | \tau_{yx} \rangle) \\ &\approx \frac{1}{2i} \nu\mu^2 \left(\frac{1}{\gamma_e + 2i\omega_c} - \frac{1}{\gamma_e - 2i\omega_c} \right) \\ &\approx \begin{cases} -\nu\mu^2 \frac{2\omega_c\gamma^{-2}}{1 + (2\omega_c\gamma^{-1})^2} & T < T_{\text{BG}} \\ -\nu\mu^2 \frac{2\omega_c\bar{\gamma}^{-2}}{1 + (2\omega_c\bar{\gamma}^{-1})^2} & T_{\text{BG}} < T \ll T_{\text{F}} \end{cases}, \end{aligned} \quad (6.6)$$

and it takes the more conventional form [40] in a Fermi liquid. Therefore, a simple test for the phonon contribution to transport and viscosity in an electron-phonon fluid would be to study the ratio

$$\mathcal{R}(B) = \frac{\eta^2 + \eta_{\text{H}}^2}{\eta}, \quad (6.7)$$

which will be a decreasing function of B because of the phonon contribution to shear viscosity.

Note that there are highly quantum effects which we have not captured in our semiclassical treatment [58].

6.2. Magnetotransport

We study the magnetotransport phenomenon by considering the strong electron phonon interaction, the impurities and the magnetic field together $\tilde{W} = W + W_{\text{imp}} + W_{\text{mag}}$. We present the results of conductivities in the limit $\Gamma_{\text{ph}} \rightarrow 0$, and we will see that this limit preserves much of the interesting quantitative behavior of conductivities, but will simplify the expressions a lot. The complete expressions can be found in Appendix D. First, we find that the electrical conductivity is given by

$$\sigma_{xx} = e^2 \frac{\nu}{2} v_{\text{F}}^2 \frac{\Gamma_e}{\Gamma_e^2 + \omega_c^2}, \quad (6.8a)$$

$$\sigma_{yx} = e^2 \frac{\nu}{2} v_{\text{F}}^2 \frac{\omega_c}{\Gamma_e^2 + \omega_c^2}. \quad (6.8b)$$

They are very similar to the form in clean Fermi liquid [41]. As discussed in the non-magnetic case, the σ_{ij} become independent of electron-phonon interactions if Γ_{ph} is negligible, and coincide with the form in the non-interacting limit (D4). The open-circuit thermal conductivities are given by ($T < T_{\text{BG}}$):

$$T\kappa_{xx} = \frac{\nu}{2} p_{\text{F}}^2 v_{\text{F}}^4 \left(\frac{\bar{a}^2 (\Gamma_e + \gamma r^2 / \bar{a}^2)}{(\Gamma_e + \gamma r^2 / \bar{a}^2)^2 + \omega_c^2} + r^4 \bar{w}^4 \gamma^{-1} \right), \quad (6.9a)$$

$$T\kappa_{yx} = \frac{\nu}{2} p_{\text{F}}^2 v_{\text{F}}^4 \frac{\bar{a}^2 \omega_c}{(\Gamma_e + \gamma r^2 / \bar{a}^2)^2 + \omega_c^2}, \quad (6.9b)$$

$$(6.9c)$$

while the closed-circuit thermal conductivities are

$$T\bar{\kappa}_{xx} = T\kappa_{xx} + \frac{\nu}{2} p_{\text{F}}^2 v_{\text{F}}^4 \frac{r^4 \bar{w}^4 \Gamma_e}{\Gamma_e^2 + \omega_c^2}, \quad (6.10a)$$

$$T\bar{\kappa}_{yx} = T\kappa_{yx} + \frac{\nu}{2} p_{\text{F}}^2 v_{\text{F}}^4 \frac{r^4 \bar{w}^4 \omega_c}{\Gamma_e^2 + \omega_c^2}. \quad (6.10b)$$

We see that in the limit $B \rightarrow 0$, the closed-circuit thermal conductivity diverges in the clean limit $\Gamma_e \rightarrow 0$ while the open-circuit thermal conductivity does not. As the Lorentz force does not act on phonon modes, one may naively think that phonon modes will not contribute to the Hall thermal conductivity. This is true for open-circuit Hall thermal conductivity, but not for closed-circuit: in the latter case, the hybrid electron-phonon fluid is charged and participates in cyclotron motion, even when the energy density of the fluid is dominated by phonons. The thermoelectric conductivity is given by ($T < T_{\text{BG}}$)

$$T\alpha_{xx} = -e \frac{\nu}{2} p_{\text{F}} v_{\text{F}}^3 \left(\frac{r^2 \bar{w}^2 \Gamma_e}{\Gamma_e^2 + \omega_c^2} + \frac{\bar{a}^2 (\Gamma_e + \gamma r^2 / \bar{a}^2)}{(\Gamma_e + \gamma r^2 / \bar{a}^2)^2 + \omega_c^2} - \bar{a} \frac{c \omega_c (2\Gamma_e + \gamma r^2 \bar{a}^2) + (b - 2\gamma r^2 / \bar{a}) (\Gamma_e^2 - \omega_c^2 + \Gamma_e \gamma r^2 / \bar{a}^2)}{((\Gamma_e + \gamma r^2 / \bar{a}^2)^2 + \omega_c^2) (\Gamma_e + \omega_c^2)} \right), \quad (6.11a)$$

$$T\alpha_{yx} = -e \frac{\nu}{2} p_{\text{F}} v_{\text{F}}^3 \left(\frac{r^2 \bar{w}^2 \omega_c}{\Gamma_e + \omega_c^2} + \frac{\bar{a}^2 \omega_c}{(\Gamma_e + \gamma r^2 / \bar{a}^2)^2 + \omega_c^2} + \bar{a} \frac{(2\gamma r^2 / \bar{a} - b) (2\Gamma_e + \gamma r^2 \bar{a}^2) \omega_c + c (\Gamma_e^2 - \omega_c^2 + \Gamma_e \gamma r^2 / \bar{a}^2)}{((\Gamma_e + \gamma r^2 / \bar{a}^2)^2 + \omega_c^2) (\Gamma_e + \omega_c^2)} \right). \quad (6.11b)$$

where c is the off-diagonal term in magnetic collision integral (D3).

We summarize the main results by studying two Lorenz numbers. The normal Lorenz number with magnetic field is given by (recovering Γ_{ph})

$$L = \frac{\kappa_{xx}}{T\sigma_{xx}} \approx \begin{cases} L_0 \left(\frac{(\Gamma_e + \gamma r^2 / \bar{a}^2)}{(\Gamma_e + \gamma r^2 / \bar{a}^2)^2 + \omega_c^2} + \frac{r^4 \bar{w}^2 / \bar{a}^2}{\Gamma_{\text{ph}} + \gamma / \bar{w}^2} \right) \frac{(\Gamma_e (\Gamma_{\text{ph}} + \gamma / \bar{w}^2) + \Gamma_{\text{ph}} \gamma)^2 + (\Gamma_{\text{ph}} + \gamma / \bar{w}^2)^2 \omega_c^2}{(\Gamma_{\text{ph}} + \gamma / \bar{w}^2) (\Gamma_e (\Gamma_{\text{ph}} + \gamma / \bar{w}^2) + \Gamma_{\text{ph}} \gamma)} & T < T_{\text{BG}} \\ L_0 \left(\frac{(\Gamma_e + \bar{\gamma})}{(\Gamma_e + \bar{\gamma})^2 + \omega_c^2} + \frac{r^4 \bar{w}^2 / \bar{a}^2}{\Gamma_{\text{ph}} + \bar{\gamma} / \bar{w}^2} \right) \frac{(\Gamma_e (\Gamma_{\text{ph}} + \bar{\gamma} / \bar{w}^2) + \Gamma_{\text{ph}} \bar{\gamma})^2 + (\Gamma_{\text{ph}} + \bar{\gamma} / \bar{w}^2)^2 \omega_c^2}{(\Gamma_{\text{ph}} + \bar{\gamma} / \bar{w}^2) (\Gamma_e (\Gamma_{\text{ph}} + \bar{\gamma} / \bar{w}^2) + \Gamma_{\text{ph}} \bar{\gamma})} & T_{\text{BG}} < T \ll T_{\text{F}} \end{cases}, \quad (6.12)$$

while the ‘‘Hall’’ Lorenz number is

$$L_{\text{H}} = \frac{\kappa_{yx}}{T\sigma_{yx}} \approx \begin{cases} L_0 \frac{(\Gamma_e (\Gamma_{\text{ph}} + \gamma / \bar{w}^2) + \Gamma_{\text{ph}} \gamma)^2 + (\Gamma_{\text{ph}} + \gamma / \bar{w}^2)^2 \omega_c^2}{((\Gamma_e + \gamma r^2 / \bar{a}^2)^2 + \omega_c^2) (\Gamma_{\text{ph}} + \gamma / \bar{w}^2)^2} & T < T_{\text{BG}} \\ L_0 \frac{(\Gamma_e (\Gamma_{\text{ph}} + \bar{\gamma} / \bar{w}^2) + \Gamma_{\text{ph}} \bar{\gamma})^2 + (\Gamma_{\text{ph}} + \bar{\gamma} / \bar{w}^2)^2 \omega_c^2}{((\Gamma_e + \bar{\gamma})^2 + \omega_c^2) (\Gamma_{\text{ph}} + \bar{\gamma} / \bar{w}^2)^2} & T_{\text{BG}} < T \ll T_{\text{F}} \end{cases}. \quad (6.13)$$

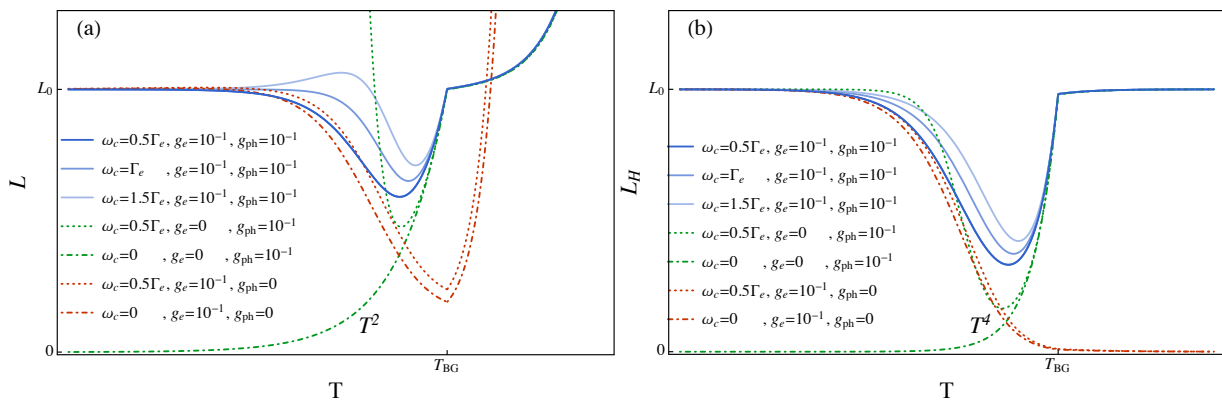


FIG. 4. (Hall) Lorenz number versus temperature with different field strengths and impurity scattering rates. For L_H , $\omega_c = 0$ really means $\omega_c \rightarrow 0$.

We show their magnetic field dependence in Figure 4. In the regime $T < T_{BG}$, we find that the L shows a non-monotonic temperature dependence when $\omega_c/\Gamma_e > 1$, similar to the interacting Fermi liquid [41], while the temperature dependence of L_H remains monotonic but with gradual growing T^* for increasing field strength. For both L and L_H , they show little dependence on B at $T > T_{BG}$, implying the phonon-dominated fluid. Taking the strict clean limit⁵, L shows a contrasting divergence in the presence of finite B at low temperature for $\Gamma_e = 0$; however, the behavior of $\Gamma_{ph} = 0$ is similar for both $B = 0$ and $B \neq 0$. By contrast, when $\Gamma_e = 0$, L_H with $B \neq 0$ ($B \rightarrow 0$) saturates to $\approx L_0$ (≈ 0 in a rate of $\sim T^4$) at low temperature. Furthermore, when $\Gamma_{ph} = 0$, L_H becomes vanishingly small at $T > T_{BG}$ for both $B \neq 0$ and $B \rightarrow 0$. However, as long as $\Gamma_{ph} \neq 0$, no matter how small it is, L_H will eventually approach L_0 at high enough temperature. We can see this from the expression that, for high enough T (if possible for $T \ll T_F$), we could have $\Gamma_{ph} \gg \bar{\gamma}/\bar{w}^2$, such that $L_H \approx L_0$. Note that we can study L_H even as $B \rightarrow 0$ (it is well-behaved when $\omega_c \rightarrow 0$), even though σ_{xy} and κ_{xy} individually become very small.

7. CONCLUSION

We have revisited the hydrodynamics and the thermoelectric transport of a fluid of coupled electrons and acoustic phonons in the presence of relatively strong electron-phonon interactions. Solving the quantum Boltzmann equation, we found 9 different temperature regimes when $d > 2$, and 7 temperature regimes for $d = 2$, most of which exhibited unconventional thermodynamic properties and/or hydrodynamic transport coefficients such as viscosity or incoherent conductivity.

An explicit and important example of unusual temperature dependence that we discovered occurs in the fluid's sound velocity. In an intermediate temperature regime $T_4 < T < T_6$, $v_s \approx v_{ph}/\bar{w} \propto T^{-(d+1)/2}$ decreases with temperature, and is a clear experimental signature for the strongly coupled electron-phonon fluid. In particular, our model implies that in two dimensions, the exotic sound wave above will lead to an unusual plasmon dispersion relation, even in the presence of unscreened (or weakly screened) long-range Coulomb interactions. The anomalous scaling of both the real and imaginary parts of $\omega_{\text{plasmon}} \sim (v_{ph}/\bar{w})\sqrt{k} - i\gamma^{-1}|k|$, represent unambiguous predictions that appear to us to be unique and “smoking gun” signatures for electron-phonon hydrodynamics. Since the real part of plasmon dispersion relations is quite readily measurable, we hope that our theory can be immediately tested with present day experimental capabilities.

Another experimental test which might be possible (indirectly) with present day experimental techniques is to look for the unusual relationships between shear viscosity and Hall viscosity, as both of these coefficients can indirectly be measured using non-local transport experiments [15, 16, 59]. Such experiments have been successfully performed in graphene [2, 7]. We hope that similar indirect measurements for incoherent conductivity can soon be developed.

After including electron-impurity and phonon-impurity scattering rates, we discussed the more conventionally studied thermoelectric transport coefficients of the bulk material. As is well known [38], we obtain a breakdown of the Wiedemann-Franz law at an intermediate temperature regime. While this effect is *not unique* to hydrodynamic theories of transport, it does represent a key signature for what temperature regime an experimental device may be

⁵ When both $\Gamma_e = \Gamma_{ph} = 0$ (hydrodynamic limit) and in the presence of finite B , L become divergent while L_H remain constant, analogous to the results of Fermi liquid [41]

operating in. In many materials including WTe_2 , WP_2 and PtSn_4 , notable dips in L/L_0 have appeared at quite low temperatures ~ 30 K. Perhaps this corresponds in these materials to the temperature range $T \sim T_4$, where the conventional electron-phonon hydrodynamics of the literature – which is entirely dominated by electrons, with phonons modifying only scattering rates – is not applicable? Especially in materials where first principles calculations [24] are possible, it will be important to carefully estimate the temperature scales T_1, \dots, T_8 in order to carefully match our theoretical predictions to future experiments.

A promising platform in realizing the simplest electron-phonon hydrodynamics developed in this paper should (at least) satisfy the conditions of low electron density and high mobility. The low density of electrons seems to demand a small Fermi surface, so that unklapp scattering is weak. At the same time, the impurity density must also be quite low, to facilitate a high mobility sample with very long momentum-relaxing mean free paths. They both contribute to the dominant momentum-conserving electron-phonon interaction. Moreover, the low density semimetal/semiconductor makes itself different from normal metal that T_{BG} drops from ~ 300 K to ~ 30 K. It is thus possible to have $T_{\text{BG}} < T_{\text{D}}$, where T_{D} is the Debye temperature, such that the phonon-drag peak temperature $\sim T_{\text{D}}/10$ [26] is more likely to be located inside the highlighted regime $T_4 < T < T_6$, indicating an out-of-equilibrium phonon mode. Such feature has been widely used in experiments [26, 60] to suggest a strong electron-phonon interaction. Meanwhile, twisted bilayer graphene [61–63] is also a possible candidate system with strong electron-phonon interactions, although in these twisted samples, the ratio r (which controlled much of the interesting physics) may become rather large. Lastly, a system where very strong electron-electron and electron-phonon interactions might both coexist is in the Si MOSFETs [64] where both T_{F} and T_{BG} can be below 30 K. Since the hybrid electron-phonon sound speed does not depend on scattering rates, being intrinsically thermodynamic, such systems may also exhibit this unusual behavior.

Our work demonstrates an exciting possibility of uncovering novel hydrodynamic phenomena and plasmonics in quantum materials with correlated electrons and phonons. We encourage experimentalists to carefully study plasmon dispersion relations in thin films of a number of compounds including PtSn_4 , PdCoO_2 , WTe_2 and WP_2 . In each of these materials, electron-phonon scattering has been argued to play a critical role in possibly unconventional transport physics. However, all of these materials exhibit anisotropic Fermi surfaces and, as in [28, 65], this anisotropy may well cause qualitative changes to our theory. This is an important issue which we hope to address in the near future.

ACKNOWLEDGEMENTS

We thank Sankar Das Sarma for useful feedback on the manuscript. AL was supported by a Research Fellowship from the Alfred P. Sloan Foundation.

Appendix A: Normalization factor of rotationally invariant basis

Following the definition in (3.15), we calculate the normalization for $n \leq 1$ to the leading order T/T_{F} . The higher n modes are suppressed by even higher powers of T/T_{F} . They are

$$\begin{aligned} \langle \tilde{0}, \mathbf{m}' | \tilde{0}, \mathbf{m} \rangle_{\text{e}} &= \int \frac{d^d p}{(2\pi\hbar)^d} Y_{\mathbf{m}} Y_{\mathbf{m}'} \left(-\frac{\partial f_{\text{F}}}{\partial \epsilon} \right) \Big|_p = \Omega_{d-1} \delta_{\mathbf{m}, \mathbf{m}'} \int \frac{d\epsilon}{(2\pi\hbar)^d v_{\text{F}}} p^{d-1} \delta(\epsilon - \mu) \\ &= \nu \delta_{\mathbf{m}, \mathbf{m}'} + \mathcal{O}\left(\frac{T^2}{T_{\text{F}}^2}\right), \end{aligned} \quad (\text{A1a})$$

$$\begin{aligned} \langle \tilde{1}, \mathbf{m}' | \tilde{1}, \mathbf{m} \rangle_{\text{e}} &= \int \frac{d^d p}{(2\pi\hbar)^d} Y_{\mathbf{m}} Y_{\mathbf{m}'} (p - p_{\text{F}})^2 \left(-\frac{\partial f_{\text{F}}}{\partial \epsilon} \right) \Big|_p = \Omega_{d-1} \delta_{\mathbf{m}, \mathbf{m}'} \int \frac{d\epsilon}{(2\pi\hbar)^d v_{\text{F}}} p^{d-1} (p - p_{\text{F}})^2 \frac{\pi^2 T^2}{3} \delta''(\epsilon - \mu) \\ &= \nu \frac{\pi^2 T^2}{3 v_{\text{F}}^2} \delta_{\mathbf{m}, \mathbf{m}'} + \mathcal{O}\left(\frac{T^4}{T_{\text{F}}^4}\right), \end{aligned} \quad (\text{A1b})$$

$$\begin{aligned} \langle \tilde{2}, \mathbf{m}' | \tilde{2}, \mathbf{m} \rangle_{\text{e}} &= \int \frac{d^d p}{(2\pi\hbar)^2} Y_{\mathbf{m}} Y_{\mathbf{m}'} (p - p_{\text{F}})^4 \left(-\frac{\partial f_{\text{F}}}{\partial \epsilon} \right) \Big|_p = \Omega_{d-1} \delta_{\mathbf{m}, \mathbf{m}'} \int \frac{d\epsilon}{(2\pi\hbar)^d v_{\text{F}}} p^{d-1} (p - p_{\text{F}})^4 \frac{7\pi^4 T^4}{180} \delta^{(4)}(\epsilon - \mu) \\ &= \mathcal{O}\left(\frac{T^4}{T_{\text{F}}^4}\right), \end{aligned} \quad (\text{A1c})$$

$$\begin{aligned}
\langle \tilde{0}, \mathbf{m}' | \tilde{1}, \mathbf{m} \rangle_e &= \int \frac{d^d p}{(2\pi\hbar)^2} Y_{\mathbf{m}} Y_{\mathbf{m}'} (p - p_F) \left(-\frac{\partial f_F}{\partial \epsilon} \right) \Big|_p = \Omega_{d-1} \delta_{\mathbf{m}, \mathbf{m}'} \int \frac{d\epsilon}{(2\pi\hbar)^d v_F} p^{d-1} (p - p_F) \frac{\pi^2 T^2}{3} \delta''(\epsilon - \mu) \\
&= \frac{\nu}{2} \frac{\pi^2 T^2}{3} \left(-\frac{\partial_p v_F}{v_F^2} \right) \delta_{\mathbf{m}, \mathbf{m}'} + \mathcal{O} \left(\frac{T^4}{T_F^4} \right),
\end{aligned} \tag{A1d}$$

$$\langle \tilde{1}, \mathbf{m}' | \tilde{1}, \mathbf{m} \rangle_{\text{ph}} = \int \frac{d^d q}{(2\pi\hbar)^d} Y_{\mathbf{m}} Y_{\mathbf{m}'} q^2 \left(-\frac{\partial f_B}{\partial \epsilon} \right) \Big|_q = \frac{\Omega_{d-1} T^{d+1} \delta_{\mathbf{m}, \mathbf{m}'}}{(2\pi\hbar)^d v_{\text{ph}}^{d+2}} \int dx \frac{x^{d+1} e^x}{(e^x - 1)^2} = 2w^2 \delta_{\mathbf{m}, \mathbf{m}'}, \tag{A1e}$$

where we define

$$I(d) = \int_0^\infty dx \frac{x^{d+1} e^x}{(e^x - 1)^2}. \tag{A2}$$

Appendix B: Explicit expressions of electron-phonon relaxation rate

First, we compute the collision integral after linearization. The zeroth-order of (3.22) vanishes due to the detailed balance condition. Notice that

$$-\frac{\partial f_F^0}{\partial \epsilon} = f_F^0 (1 - f_F^0), \quad -\frac{\partial f_B^0}{\partial \epsilon} = b_B^0 (1 + b_B^0). \tag{B1}$$

Then the first-order of $\mathcal{C}_{\text{ph-e}}$ becomes

$$\begin{aligned}
T \delta \mathcal{C}_{\text{e-ph}} &= \{ f_{Fk_2} (1 - f_{Fk_2}) (1 - f_{Fk_1}) (1 + b_{Bq}) + f_{Fk_1} f_{Fk_2} (1 - f_{Fk_2}) b_{Bq} \} \Phi_{k_2} \\
&\quad + \{ -f_{Fk_2} f_{Fk_1} (1 - f_{Fk_1}) (1 + b_{Bq}) - f_{Fk_1} (1 - f_{Fk_1}) (1 - f_{Fk_2}) b_{Bq} \} \Phi_{k_1} \\
&\quad + \{ f_{Fk_2} (1 - f_{Fk_1}) b_{Bq} (1 + b_{Bq}) - f_{Fk_1} (1 - f_{Fk_2}) b_{Bq} (1 + b_{Bq}) \} \Phi_q \\
&= (1 - f_{Fk_2}) f_{Fk_1} b_{Bq} (\Phi_{k_2} - \Phi_{k_1}) + (f_{Fk_2} - f_{Fk_1}) b_{Bq} (1 + b_{Bq}) \Phi_q \\
&= (1 - f_{Fk_2}) f_{Fk_1} b_{Bq} (\Phi_{k_2} - \Phi_{k_1} - \Phi_q),
\end{aligned} \tag{B2}$$

where in the last equation, we use the energy conservation. (3.24) is obtained straightforwardly.

Next, we want to calculate the scaling on temperature of the collision integral. Based on the discussion below (3.24), we separate our discussions into two temperature regimes: $T < T_{\text{BG}}$ and $T > T_{\text{BG}}$.

1. $T < T_{\text{BG}}$

We evaluate (3.24) in a general ground by assuming Φ 's being ϵ -dependent.

$$\begin{aligned}
\langle \Phi | W_{\text{e-ph}} | \Phi \rangle &\approx \beta \int_{\mathbf{q}, \mathbf{k}_1, \mathbf{k}_2} |A|^2 \delta(\mathbf{k}_2 - \mathbf{k}_1 - \mathbf{q}) \delta(\epsilon_{k_2} - \epsilon_{k_1} - \omega_q) (1 - f_{\text{F}k_2}) f_{\text{F}k_1} f_{\text{B}q} |\Phi|^2 \\
&= \int_{\mathbf{q}} \int \frac{d\epsilon_2}{|v(\mathbf{k}_2)|} \frac{d^{d-1}k_{\parallel}}{(2\pi)^d} \beta |A|^2 \delta(\epsilon_{k_2} - \epsilon_{k_2-q} - \omega_q) (1 - f_{\text{F}k_2}) f_{\text{F}k_2-q} f_{\text{B}q} |\Phi|^2 \\
&= \int_{\mathbf{q}} \int \frac{d\epsilon_2}{|v(\mathbf{k}_2)|} \frac{d^{d-1}k_{\parallel}}{(2\pi)^d} |A|^2 \delta(\epsilon_{k_2} - \epsilon_{k_2-q} - \omega_q) \beta (1 - f_{\text{F}k_2}) \frac{f_{\text{F}k_2-q}}{f_{\text{F}k_2}} f_{\text{B}q} |\Phi|^2 \\
&= \int_{\mathbf{q}} \int \frac{d\epsilon_2}{|v(\mathbf{k}_2)|} \frac{d^{d-1}k_{\parallel}}{(2\pi)^d} |A|^2 \delta(\epsilon_{k_2} - \epsilon_{k_2-q} - \omega_q) (\delta(\epsilon_2 - \mu) + \frac{\pi^2 T^2}{3} \delta''(\epsilon_2 - \mu) + \dots) \frac{f_{\text{F}k_2-q}}{f_{\text{F}k_2}} f_{\text{B}q} |\Phi|^2 \\
&= \int_{\mathbf{q}} \int \frac{d^{d-1}k_{\parallel}}{(2\pi)^d v_{\text{F}}} D_{\text{e-ph}} |\mathbf{q}| \frac{\delta(\cos \theta_{\mathbf{q}\mathbf{k}_{\parallel}} - v_{\text{ph}}/v_{\text{F}})}{v_{\text{F}} q} \frac{2}{e^{-\beta\omega} + 1} \frac{1}{e^{\beta\omega} - 1} \int d\epsilon_2 (\delta(\epsilon_2 - \mu) + \frac{\pi^2 T^2}{3} \delta''(\epsilon_2 - \mu) + \dots) |\Phi|^2 \\
&= D_{\text{e-ph}} \int_{\mathbf{q}} \int \frac{d^{d-1}k_{\parallel}}{(2\pi)^d v_{\text{F}}^2} \delta(\cos \theta_{\mathbf{q}\mathbf{k}_{\parallel}} - v_{\text{ph}}/v_{\text{F}}) \frac{1}{\sinh(\beta\omega)} \int d\epsilon_2 (\delta(\epsilon_2 - \mu) + \frac{\pi^2 T^2}{3} \delta''(\epsilon_2 - \mu) + \dots) |\Phi|^2 \\
&\approx D_{\text{e-ph}} \int_{\mathbf{q}} \int \frac{d^{d-1}\mathbf{k}_{\parallel}}{(2\pi)^d v_{\text{F}}^2} \delta(\cos \theta_{\mathbf{q}\mathbf{k}_{\parallel}} - v_{\text{ph}}/v_{\text{F}}) \times \Theta(T - v_{\text{ph}}q) \int d\epsilon_2 (\delta(\epsilon_2 - \mu) + \frac{\pi^2 T^2}{3} \delta''(\epsilon_2 - \mu) + \dots) |\Phi|^2 \\
&= D_{\text{e-ph}} \int_0^{T/v_{\text{ph}}} \frac{d^d q}{(2\pi)^d} \int \frac{d^{d-1}k_{\parallel}}{(2\pi)^d v_{\text{F}}^2} \delta(\cos \theta_{\mathbf{q}\mathbf{k}_{\parallel}} - v_{\text{ph}}/v_{\text{F}}) \int d\epsilon_2 (\delta(\epsilon_2 - \mu) + \frac{\pi^2 T^2}{3} \delta''(\epsilon_2 - \mu) + \dots) |\Phi|^2
\end{aligned} \tag{B3}$$

We find that $\theta_{\mathbf{q}\mathbf{k}_{\parallel}} \approx \pi/2$ implying that phonon momentum is approximately perpendicular to electron momentum. We then apply the ‘‘Bloch Ansatz’’ $|\Phi\rangle_{\text{ph}} = 0$, and replacing the $|\Phi\rangle$ mode with rotationally invariant basis. We have

$${}_{\text{e}}\langle \tilde{0} | W_{\text{e-ph}} | \tilde{0} \rangle_{\text{e}} \approx D_{\text{e-ph}} \int_0^{T/v_{\text{ph}}} \frac{d^d q}{(2\pi)^d} \int \frac{d^{d-1}k_{\parallel}}{(2\pi)^d v_{\text{F}}^2} \delta(\cos \theta_{\mathbf{q}\mathbf{k}_{\parallel}} - v_{\text{ph}}/v_{\text{F}}) \frac{q^2}{p_{\text{F}}^2} = \alpha^2(2) \frac{1}{p_{\text{F}}^2} T^{d+2}, \tag{B4a}$$

$${}_{\text{e}}\langle \tilde{1} | W_{\text{e-ph}} | \tilde{1} \rangle_{\text{e}} \approx D_{\text{e-ph}} \int_0^{T/v_{\text{ph}}} \frac{d^d q}{(2\pi)^d} \int \frac{d^{d-1}k_{\parallel}}{(2\pi)^d v_{\text{F}}^2} \delta(\cos \theta_{\mathbf{q}\mathbf{k}_{\parallel}} - v_{\text{ph}}/v_{\text{F}}) \frac{v_{\text{ph}}^2}{v_{\text{F}}^2} q^2 = \alpha^2(2) \frac{v_{\text{ph}}^2}{v_{\text{F}}^2} T^{d+2}, \tag{B4b}$$

$${}_{\text{e}}\langle \tilde{2} | W_{\text{e-ph}} | \tilde{2} \rangle_{\text{e}} \approx D_{\text{e-ph}} \int_0^{T/v_{\text{ph}}} \frac{d^d q}{(2\pi)^d} \int \frac{d^{d-1}k_{\parallel}}{(2\pi)^d v_{\text{F}}^2} \delta(\cos \theta_{\mathbf{q}\mathbf{k}_{\parallel}} - v_{\text{ph}}/v_{\text{F}}) \frac{v_{\text{ph}}^4}{v_{\text{F}}^4} q^4 = \alpha^2(4) \frac{v_{\text{ph}}^4}{v_{\text{F}}^4} T^{d+4}, \tag{B4c}$$

where

$$\alpha^2(n) = D_{\text{e-ph}} \int_0^1 \frac{d^d x x^n}{(2\pi)^d} \int \frac{d^{d-1}k_{\parallel}}{(2\pi)^d v_{\text{F}}^2 v_{\text{ph}}^{d+n}} \delta(\cos \theta_{\mathbf{x}\mathbf{k}_{\parallel}} - v_{\text{ph}}/v_{\text{F}}). \tag{B5}$$

To derive the relaxation time for phonons, we set $\Phi_{\text{e}} = 0$. Then the collision integral for phonon modes is given by

$${}_{\text{ph}}\langle \tilde{1} | W_{\text{e-ph}} | \tilde{1} \rangle_{\text{ph}} \approx D_{\text{e-ph}} \int_0^{T/v_{\text{ph}}} \frac{d^d q}{(2\pi)^d} \int \frac{d^{d-1}k_{\parallel}}{(2\pi)^d v_{\text{F}}^2} \delta(\cos \theta_{\mathbf{q}\mathbf{k}_{\parallel}} - v_{\text{ph}}/v_{\text{F}}) (q\hat{q})^2 = \alpha^2(2) T^{d+2}. \tag{B6}$$

2. $T > T_{\text{BG}}$

We need to recalculate the collision integral (B3), and this time the phonon behaves more like a classical boson gas with equipartition distribution:

$$\begin{aligned}
\langle \Phi | W_{\text{e-ph}} | \Phi \rangle &\approx \int_{\mathbf{q}} \int \frac{d^{d-1}k_{\parallel}}{(2\pi)^d v_{\text{F}}} |A|^2 \delta(\epsilon_{k_2} - \epsilon_{k_2-q} - \omega_q) \frac{1}{\sinh(\beta\omega_q)} \int d\epsilon_2 (\delta(\epsilon_2 - \mu) + \frac{\pi^2 T^2}{3} \delta''(\epsilon_2 - \mu) + \dots) |\Phi|^2 \\
&\approx D_{\text{e-ph}} \int^{k_{\text{F}}} \frac{d^d q}{(2\pi)^d} \int \frac{d^{d-1}k_{\parallel}}{(2\pi)^d v_{\text{F}}} \delta(\epsilon_{k_2} - \epsilon_{k_2-q} - \omega_q) \frac{T}{v_{\text{ph}}} \int d\epsilon_2 (\delta(\epsilon_2 - \mu) + \frac{\pi^2 T^2}{3} \delta''(\epsilon_2 - \mu) + \dots) |\Phi|^2.
\end{aligned} \tag{B7}$$

We apply $|\Phi\rangle_{\text{ph}} = 0$, and find

$${}_e\langle\tilde{0}|W_{\text{e-ph}}|\tilde{0}\rangle_e \approx D_{\text{e-ph}} \int^{k_F} \frac{d^d q}{(2\pi)^d} \int \frac{d^{d-1} k_{\parallel}}{(2\pi)^d v_F} \delta(\epsilon_{k_2} - \epsilon_{k_2-q} - \omega_q) \frac{T}{v_{\text{ph}} p_F^2} = \alpha'^2(2) \frac{1}{p_F^2} T, \quad (\text{B8a})$$

$${}_e\langle\tilde{1}|W_{\text{e-ph}}|\tilde{1}\rangle_e \approx D_{\text{e-ph}} \int^{k_F} \frac{d^d q}{(2\pi)^d} \int \frac{d^{d-1} k_{\parallel}}{(2\pi)^d v_F} \delta(\epsilon_{k_2} - \epsilon_{k_2-q} - \omega_q) \frac{T}{v_{\text{ph}}} a^2 \approx \alpha'^2(2) \frac{a^2}{p_F^2} T, \quad (\text{B8b})$$

where

$$\alpha'^2(n) = D_{\text{e-ph}} \int^{k_F} \frac{d^d q}{(2\pi)^d} \int \frac{d^{d-1} k_{\parallel}}{(2\pi)^d v_F} \delta(\epsilon_{k_2} - \epsilon_{k_2-q} - \omega_q) \frac{q^n}{v_{\text{ph}}}. \quad (\text{B9})$$

If we apply $|\Phi\rangle_e = 0$, we have

$${}_{\text{ph}}\langle\tilde{1}|W_{\text{e-ph}}|\tilde{1}\rangle_{\text{ph}} \approx D_{\text{e-ph}} \int^{k_F} \frac{d^d q}{(2\pi)^d} \int \frac{d^{d-1} k_{\parallel}}{(2\pi)^d v_F} \delta(\epsilon_{k_2} - \epsilon_{k_2-q} - \omega_q) \frac{T}{v_{\text{ph}}} q^2 = \alpha'^2(2) T. \quad (\text{B10})$$

Appendix C: Matrix elements of collision integrals without magnetic field

According to (3.28), we have

$$W'_{\text{e-ph}} = \begin{pmatrix} \bar{a}^2 + \bar{w}^2 & -\bar{a} & -\bar{w} \\ -\bar{a} & 1 + \bar{w}^2 & -\bar{a}\bar{w} \\ -\bar{w} & -\bar{a}\bar{w} & 1 + \bar{a}^2 \end{pmatrix} \frac{W_{\text{e-ph}}}{(1 + \bar{a}^2 + \bar{w}^2)^2} \begin{pmatrix} \bar{a}^2 + \bar{w}^2 & -\bar{a} & -\bar{w} \\ -\bar{a} & 1 + \bar{w}^2 & -\bar{a}\bar{w} \\ -\bar{w} & -\bar{a}\bar{w} & 1 + \bar{a}^2 \end{pmatrix}. \quad (\text{C1})$$

We write

$$W = W_{\text{imp}}^{\text{e}} + W_{\text{imp}}^{\text{ph}} + W'_{\text{e-ph}} = \begin{pmatrix} A_1 & A_4 & A_5 \\ A_4 & A_2 & A_6 \\ A_5 & A_6 & A_3 \end{pmatrix}, \quad (\text{C2})$$

where for $T < T_{\text{BG}}$,

$$A_1 = \Gamma_e + \gamma \frac{(1 + r^2 + (\bar{a}^2 + \bar{w}^2)^2)}{(1 + \bar{a}^2 + \bar{w}^2)^2}, \quad (\text{C3a})$$

$$A_2 = \Gamma_e + \gamma \frac{r^2(1 + \bar{w}^2)^2}{\bar{a}^2(1 + \bar{a}^2 + \bar{w}^2)^2}, \quad (\text{C3b})$$

$$A_3 = \Gamma_{\text{ph}} + \gamma \frac{((1 + \bar{a}^2)^2 + \bar{w}^4)}{\bar{w}^2(1 + \bar{a}^2 + \bar{w}^2)^2}, \quad (\text{C3c})$$

$$A_4 = b - \gamma \frac{\bar{a}^2(-1 + \bar{w}^2) + r^2(1 + \bar{w}^2)}{\bar{a}(1 + \bar{a}^2 + \bar{w}^2)^2}, \quad (\text{C3d})$$

$$A_5 = -\gamma \frac{1 + (\bar{a}^2 - r^2)\bar{w}^2 + \bar{w}^4}{\bar{w}(1 + \bar{a}^2 + \bar{w}^2)^2}, \quad (\text{C3e})$$

$$A_6 = \gamma \frac{\bar{a}^2(-1 + \bar{w}^2) - r^2(1 + \bar{w}^2)}{\bar{a}\bar{w}(1 + \bar{a}^2 + \bar{w}^2)^2}, \quad (\text{C3f})$$

and for $T > T_{\text{BG}}$,

$$A_1 = \Gamma_e + \bar{\gamma} \frac{(1 + \bar{a}^4 + \bar{w}^4 + \bar{a}^2(1 + 2\bar{w}^2))}{(1 + \bar{a}^2 + \bar{w}^2)^2}, \quad (\text{C4a})$$

$$A_2 = \Gamma_e + \bar{\gamma} \frac{2\bar{a}^2 + (1 + \bar{w}^2)^2}{(1 + \bar{a}^2 + \bar{w}^2)^2}, \quad (\text{C4b})$$

$$A_3 = \Gamma_{\text{ph}} + \bar{\gamma} \frac{(1 + \bar{a}^2)(1 + \bar{a}^2 + \bar{w}^4)}{\bar{w}^2(1 + \bar{a}^2 + \bar{w}^2)^2}, \quad (\text{C4c})$$

$$A_4 = b - \bar{\gamma} \frac{\bar{a}(\bar{a}^2 + 2\bar{w}^2)}{(1 + \bar{a}^2 + \bar{w}^2)^2}, \quad (\text{C4d})$$

$$A_5 = -\bar{\gamma} \frac{1 + \bar{a}^2 + \bar{w}^4}{\bar{w}(1 + \bar{a}^2 + \bar{w}^2)^2}, \quad (\text{C4e})$$

$$A_6 = \bar{\gamma} \frac{\bar{a}(1 + \bar{a}^2 + \bar{w}^4)}{\bar{w}(1 + \bar{a}^2 + \bar{w}^2)^2}. \quad (\text{C4f})$$

The inverse of W matrix is given by

$$W^{-1} = D^{-1} \begin{pmatrix} A_2 A_3 - A_6^2 & -A_3 A_4 + A_5 A_6 & -A_2 A_5 + A_4 A_6 \\ -A_3 A_4 + A_5 A_6 & A_1 A_3 - A_5^2 & A_4 A_5 - A_1 A_6 \\ -A_2 A_5 + A_4 A_6 & A_4 A_5 - A_1 A_6 & A_1 A_2 - A_4^2 \end{pmatrix}, \quad (\text{C5})$$

where

$$D = \det W = A_1 A_2 A_3 - A_3 A_4^2 - A_2 A_5^2 + 2A_4 A_5 A_6 - A_1 A_6^2. \quad (\text{C6})$$

We then approximate the W^{-1} in the above two temperature regimes.

At $T < T_{\text{BG}}$ we have the determinant

$$D \approx (\Gamma_e + r^2 \gamma / \bar{a}^2) [\Gamma_e (\Gamma_{\text{ph}} + \gamma / \bar{w}^2) + \Gamma_{\text{ph}} \gamma], \quad (\text{C7})$$

and the collision integral becomes

$$W^{-1} \approx \begin{pmatrix} \frac{\Gamma_{\text{ph}} + \gamma / \bar{w}^2}{\Gamma_e (\Gamma_{\text{ph}} + \gamma / \bar{w}^2) + \Gamma_{\text{ph}} \gamma} & \frac{-(\Gamma_{\text{ph}} + \gamma / \bar{w}^2)(b - \gamma r^2 / \bar{a}) + \gamma^2 r^2 / (\bar{a} \bar{w}^2)}{D} & \frac{\gamma / \bar{w}}{\Gamma_e (\Gamma_{\text{ph}} + \gamma / \bar{w}^2) + \Gamma_{\text{ph}} \gamma} \\ \frac{-(\Gamma_{\text{ph}} + \gamma / \bar{w}^2)(b - \gamma r^2 / \bar{a}) + \gamma^2 r^2 / (\bar{a} \bar{w}^2)}{D} & \frac{1}{\Gamma_e + r^2 \gamma / \bar{a}^2} & \frac{-(b - \gamma r^2 / \bar{a}) \gamma / \bar{w} + (\Gamma_e + \gamma) \gamma r^2 / (\bar{a} \bar{w})}{D} \\ \frac{\gamma / \bar{w}}{\Gamma_e (\Gamma_{\text{ph}} + \gamma / \bar{w}^2) + \Gamma_{\text{ph}} \gamma} & \frac{-(b - \gamma r^2 / \bar{a}) \gamma / \bar{w} + (\Gamma_e + \gamma) \gamma r^2 / (\bar{a} \bar{w})}{D} & \frac{\Gamma_e + \gamma}{\Gamma_e (\Gamma_{\text{ph}} + \gamma / \bar{w}^2) + \Gamma_{\text{ph}} \gamma} \end{pmatrix}, \quad (\text{C8})$$

while at $T > T_{\text{BG}}$ we have the determinant

$$D \approx (\Gamma_e + \bar{\gamma}) [\Gamma_e (\Gamma_{\text{ph}} + \bar{\gamma} / \bar{w}^2) + \Gamma_{\text{ph}} \bar{\gamma}], \quad (\text{C9})$$

and the collision integral becomes

$$W^{-1} \approx \begin{pmatrix} \frac{\Gamma_{\text{ph}} + \bar{\gamma} / \bar{w}^2}{\Gamma_e (\Gamma_{\text{ph}} + \bar{\gamma} / \bar{w}^2) + \Gamma_{\text{ph}} \bar{\gamma}} & \frac{-(\Gamma_{\text{ph}} + \bar{\gamma} / \bar{w}^2)(b - \bar{\gamma} \bar{a}) + \bar{\gamma}^2 \bar{a} / \bar{w}^2}{D} & \frac{\bar{\gamma} / \bar{w}}{\Gamma_e (\Gamma_{\text{ph}} + \bar{\gamma} / \bar{w}^2) + \Gamma_{\text{ph}} \bar{\gamma}} \\ \frac{-(\Gamma_{\text{ph}} + \bar{\gamma} / \bar{w}^2)(b - \bar{\gamma} \bar{a}) + \bar{\gamma}^2 \bar{a} / \bar{w}^2}{D} & \frac{1}{\Gamma_e + \bar{\gamma}} & \frac{-(b - \bar{\gamma} \bar{a}) \bar{\gamma} / \bar{w} + (\Gamma_e + \bar{\gamma}) \bar{\gamma} \bar{a} / \bar{w}}{D} \\ \frac{\bar{\gamma} / \bar{w}}{\Gamma_e (\Gamma_{\text{ph}} + \bar{\gamma} / \bar{w}^2) + \Gamma_{\text{ph}} \bar{\gamma}} & \frac{-(b - \bar{\gamma} \bar{a}) \bar{\gamma} / \bar{w} + (\Gamma_e + \bar{\gamma}) \bar{\gamma} \bar{a} / \bar{w}}{D} & \frac{\Gamma_e + \bar{\gamma}}{\Gamma_e (\Gamma_{\text{ph}} + \bar{\gamma} / \bar{w}^2) + \Gamma_{\text{ph}} \bar{\gamma}} \end{pmatrix}. \quad (\text{C10})$$

In above equations, we keep the leading order in T/T_{F} .

Appendix D: Matrix elements of collision integrals with magnetic field

We consider only $|0_{x,y}\rangle_e$, $|1_{x,y}\rangle_e$ and $|1_{x,y}\rangle_{\text{ph}}$ to keep track of the leading order temperature dependence of all conductivities. Here the integers correspond to the radial modes (not the angular modes). We focus on $d = 2$ spatial dimensions. We write

$$\tilde{W} = W \otimes \delta_{ij} + \tilde{W}_{\text{mag}} \otimes \epsilon_{ij}, \quad (\text{D1})$$

where

$$\tilde{W}_{\text{mag}} = \omega_c (|0\rangle_e \langle 0|_e + |1\rangle_e \langle 1|_e) + c (|0\rangle_e \langle 1|_e + |1\rangle_e \langle 0|_e), \quad (\text{D2})$$

and

$$c = \frac{\pi T e B (p_{\text{F}} \partial_p v_{\text{F}} - v_{\text{F}})}{\sqrt{3} v_{\text{F}} p_{\text{F}}}. \quad (\text{D3})$$

Using (D1), we are allowed to invert the 6×6 collision matrix to calculate the conductivities.

let's begin by studying the non-interacting limit $\gamma \rightarrow 0$. After some algebra, we have

$$\sigma_{xx} \approx e^2 \frac{\nu}{2} v_F^2 \frac{\Gamma_e}{\Gamma_e^2 + \omega_c^2}, \quad (D4a)$$

$$\sigma_{yx} \approx e^2 \frac{\nu}{2} v_F^2 \frac{\omega_c}{\Gamma_e^2 + \omega_c^2}, \quad (D4b)$$

$$T\kappa_{xx} \approx T\bar{\kappa}_{xx} \approx \frac{\nu}{2} p_F^2 v_F^4 \left(\frac{\bar{a}^2 \Gamma_e}{\Gamma_e^2 + \omega_c^2} + \frac{r^4 \bar{\omega}^2}{\Gamma_{ph}} \right), \quad (D4c)$$

$$T\kappa_{yx} \approx T\bar{\kappa}_{yx} \approx \frac{\nu}{2} p_F^2 v_F^4 \frac{\bar{a}^2 \omega_c}{\Gamma_e^2 + \omega_c^2}, \quad (D4d)$$

$$T\alpha_{xx} \approx -e \frac{\nu}{2} p_F v_F^3 \left(\frac{\bar{a}^2 \Gamma_e}{\Gamma_e^2 + \omega_c^2} - \bar{a} \frac{b(\Gamma_e^2 - \omega_c^2) + 2c\Gamma_e \omega_c}{(\Gamma_e^2 + \omega_c^2)^2} \right), \quad (D4e)$$

$$T\alpha_{yx} \approx -e \frac{\nu}{2} p_F v_F^3 \left(\frac{\bar{a}^2 \omega_c}{\Gamma_e^2 + \omega_c^2} + \bar{a} \frac{c(\Gamma_e^2 - \omega_c^2) - 2b\Gamma_e \omega_c}{(\Gamma_e^2 + \omega_c^2)^2} \right). \quad (D4f)$$

In above equations, we keep the leading order in the limit $T \rightarrow 0$. They are well reduced to the non-magnetic cases as discussed in the main text. We see that only (non-Hall) thermal conductivity receives a phonon's contribution which is totally B -irrelevant. This leads to two consequences. First, for a large enough B , phonon modes will dominate the thermal conductivity; Second, in the clean limit $\Gamma_{e,ph} \rightarrow 0$, the divergence shows up in thermal conductivity through the phonon modes.

Including the momentum-conserving electron-phonon interaction, we obtain at $T < T_{BG}$,

$$\sigma_{xx} \approx e^2 \frac{\nu}{2} v_F^2 \frac{(\gamma + \Gamma_{ph} \bar{\omega}^2)(\gamma \Gamma_e + (\gamma + \Gamma_e) \Gamma_{ph} \bar{\omega}^2)}{\gamma^2 (\Gamma_e^2 + \omega_c^2) + 2\gamma \Gamma_{ph} (\Gamma_e (\gamma + \Gamma_e) + \omega_c^2) \bar{\omega}^2 + \Gamma_{ph}^2 ((\gamma + \Gamma_e)^2 + \omega_c^2) \bar{\omega}^4}, \quad (D5a)$$

$$\sigma_{yx} \approx e^2 \frac{\nu}{2} v_F^2 \frac{\omega_c (\gamma + \Gamma_{ph} \bar{\omega}^2)^2}{\gamma^2 (\Gamma_e^2 + \omega_c^2) + 2\gamma \Gamma_{ph} (\Gamma_e (\gamma + \Gamma_e) + \omega_c^2) \bar{\omega}^2 + \Gamma_{ph}^2 ((\gamma + \Gamma_e)^2 + \omega_c^2) \bar{\omega}^4}, \quad (D5b)$$

$$T\bar{\kappa}_{xx} \approx \frac{\nu}{2} p_F^2 v_F^4 \left(\frac{(\bar{a}^2 \Gamma_e + r^2 \gamma)}{\Gamma_e^2 + \omega_c^2 + 2\Gamma_e \gamma r^2 / \bar{a}^2 + \gamma^2 r^4 / \bar{a}^4} + \frac{r^4 \bar{\omega}^2 (\bar{\omega}^2 \gamma [\Gamma_e (\gamma + \Gamma_e) + \omega_c^2] + \bar{\omega}^4 \Gamma_{ph} [(\gamma + \Gamma_e)^2 + \omega_c^2])}{\gamma^2 (\Gamma_e^2 + \omega_c^2) + 2\gamma \Gamma_{ph} (\Gamma_e (\gamma + \Gamma_e) + \omega_c^2) \bar{\omega}^2 + \Gamma_{ph}^2 ((\gamma + \Gamma_e)^2 + \omega_c^2) \bar{\omega}^4} \right), \quad (D5c)$$

$$T\bar{\kappa}_{yx} \approx \frac{\nu}{2} p_F^2 v_F^4 \left(\frac{\omega_c \bar{a}^2}{(\Gamma_e^2 + \omega_c^2) + 2\Gamma_e \gamma r^2 / \bar{a}^2 + \gamma^2 r^4 / \bar{a}^4} + \frac{r^4 \bar{\omega}^4 \gamma^2 \omega_c}{\gamma^2 (\Gamma_e^2 + \omega_c^2) + 2\gamma \Gamma_{ph} (\Gamma_e (\gamma + \Gamma_e) + \omega_c^2) \bar{\omega}^2 + \Gamma_{ph}^2 ((\gamma + \Gamma_e)^2 + \omega_c^2) \bar{\omega}^4} \right), \quad (D5d)$$

$$T\alpha_{xx} \approx -e \frac{\nu}{2} p_F v_F^3 \left(\frac{\gamma r^2 \bar{\omega}^2 (\gamma \Gamma_e + (\gamma + \Gamma_e) \Gamma_{ph} \bar{\omega}^2)}{\gamma^2 (\Gamma_e^2 + \omega_c^2) + 2\gamma \Gamma_{ph} (\Gamma_e (\gamma + \Gamma_e) + \omega_c^2) \bar{\omega}^2 + \Gamma_{ph}^2 ((\gamma + \Gamma_e)^2 + \omega_c^2) \bar{\omega}^4} + \frac{(\bar{a}^2 \Gamma_e + r^2 \gamma)}{\Gamma_e^2 + \omega_c^2 + 2\Gamma_e \gamma r^2 / \bar{a}^2 + \gamma^2 r^4 / \bar{a}^4} \right) \quad (D5e)$$

$$+ \frac{\bar{a}}{((\Gamma_e + \gamma r^2 / \bar{a}^2)^2 + \omega_c^2) ((\gamma \Gamma_e + \Gamma_{ph} (\gamma + \Gamma_e) \bar{\omega}^2)^2 + \omega_c^2 (\gamma + \Gamma_{ph} \bar{\omega}^2)^2)}$$

$$\times \left\{ (\gamma + \Gamma_{ph} \bar{\omega}^2) [-c(2\gamma \Gamma_e \omega_c + \Gamma_{ph} (\gamma + 2\Gamma_e) \omega_c \bar{\omega}^2) + b(\gamma (-\Gamma_e^2 + \omega_c^2) + \Gamma_{ph} (-\Gamma_e (\gamma + \Gamma_e) + \omega_c^2) \bar{\omega}^2)] \right.$$

$$- \gamma r^2 / \bar{a}^2 [c\omega_c (\gamma + \Gamma_{ph})^2 + b(\gamma^2 \Gamma_e + \gamma \Gamma_{ph} (\gamma + 2\Gamma_e) \bar{\omega}^2 + \Gamma_{ph}^2 (\gamma + \Gamma_e) \bar{\omega}^4)]$$

$$- \bar{a} \gamma r^2 / \bar{a}^2 (2\gamma + \Gamma_{ph} \bar{\omega}^2) [\gamma (-\Gamma_e^2 + \omega_c^2) + \Gamma_{ph} (-\Gamma_e (\gamma + \Gamma_e) + \omega_c^2) \bar{\omega}^2]$$

$$\left. + \bar{a} \gamma^2 r^4 / \bar{a}^4 (2\gamma + \Gamma_{ph} \bar{\omega}^2) [\Gamma_e \Gamma_{ph} \bar{\omega}^2 + \gamma (\Gamma_e + \Gamma_{ph} \bar{\omega}^2)] \right\},$$

$$T\alpha_{yx} \approx -e \frac{\nu}{2} p_F v_F^3 \left(\frac{\omega_c \gamma r^2 \bar{\omega}^2 (\gamma + \Gamma_{ph} \bar{\omega}^2)}{\gamma^2 (\Gamma_e^2 + \omega_c^2) + 2\gamma \Gamma_{ph} (\Gamma_e (\gamma + \Gamma_e) + \omega_c^2) \bar{\omega}^2 + \Gamma_{ph}^2 ((\gamma + \Gamma_e)^2 + \omega_c^2) \bar{\omega}^4} + \frac{\omega_c \bar{a}^2}{(\Gamma_e^2 + \omega_c^2) + 2\Gamma_e \gamma r^2 / \bar{a}^2 + \gamma^2 r^4 / \bar{a}^4} \right) \quad (D5f)$$

$$+ \frac{\bar{a}}{((\Gamma_e + \gamma r^2 / \bar{a}^2)^2 + \omega_c^2) ((\gamma \Gamma_e + \Gamma_{ph} (\gamma + \Gamma_e) \bar{\omega}^2)^2 + \omega_c^2 (\gamma + \Gamma_{ph} \bar{\omega}^2)^2)}$$

$$\begin{aligned} & \times \left\{ (\gamma + \Gamma_{\text{ph}}\bar{w}^2) [-b(2\gamma\Gamma_e\omega_c + \Gamma_{\text{ph}}(\gamma + 2\Gamma_e)\omega_c\bar{w}^2) - c(\gamma(-\Gamma_e^2 + \omega_c^2) + \Gamma_{\text{ph}}(-\Gamma_e(\gamma + \Gamma_e) + \omega_c^2)\bar{w}^2)] \right. \\ & - \gamma r^2/\bar{a}^2 [b\omega_c(\gamma + \Gamma_{\text{ph}})^2 - c(\gamma^2\Gamma_e + \gamma\Gamma_{\text{ph}}(\gamma + 2\Gamma_e)\bar{w}^2 + \Gamma_{\text{ph}}^2(\gamma + \Gamma_e)\bar{w}^4)] \\ & + \bar{a}\gamma r^2/\bar{a}^2\omega_c(2\gamma + \Gamma_e\bar{w}^2)(2\gamma\Gamma_e + (\gamma + 2\Gamma_e)\Gamma_{\text{ph}}\bar{w}^2) \\ & \left. + \bar{a}\gamma^2 r^4/\bar{a}^4\omega_c(2\gamma + \Gamma_{\text{ph}}\bar{w}^2)(\gamma + \Gamma_{\text{ph}}\bar{w}^2) \right\}, \end{aligned}$$

and at $T > T_{\text{BG}}$,

$$\sigma_{xx} \approx e^2 \frac{\nu}{2} v_{\text{F}}^2 \frac{(\bar{\gamma} + \Gamma_{\text{ph}}\bar{w}^2)(\bar{\gamma}\Gamma_e + (\bar{\gamma} + \Gamma_e)\Gamma_{\text{ph}}\bar{w}^2)}{\bar{\gamma}^2(\Gamma_e^2 + \omega_c^2) + 2\bar{\gamma}\Gamma_{\text{ph}}(\Gamma_e(\bar{\gamma} + \Gamma_e) + \omega_c^2)\bar{w}^2 + \Gamma_{\text{ph}}^2((\bar{\gamma} + \Gamma_e)^2 + \omega_c^2)\bar{w}^4}, \quad (\text{D6a})$$

$$\sigma_{yx} \approx e^2 \frac{\nu}{2} v_{\text{F}}^2 \frac{\omega_c(\bar{\gamma} + \Gamma_{\text{ph}}\bar{w}^2)^2}{\bar{\gamma}^2(\Gamma_e^2 + \omega_c^2) + 2\bar{\gamma}\Gamma_{\text{ph}}(\Gamma_e(\bar{\gamma} + \Gamma_e) + \omega_c^2)\bar{w}^2 + \Gamma_{\text{ph}}^2((\bar{\gamma} + \Gamma_e)^2 + \omega_c^2)\bar{w}^4}, \quad (\text{D6b})$$

$$T\bar{\kappa}_{xx} \approx \frac{\nu}{2} p_{\text{F}}^2 v_{\text{F}}^4 \left(\frac{\bar{a}^2(\Gamma_e + \bar{\gamma})}{\Gamma_e^2 + \omega_c^2 + 2\Gamma_e\bar{\gamma} + \bar{\gamma}^2} + \frac{r^4\bar{w}^2(\bar{w}^2\bar{\gamma}[\Gamma_e(\bar{\gamma} + \Gamma_e) + \omega_c^2] + \bar{w}^4\Gamma_{\text{ph}}[(\bar{\gamma} + \Gamma_e)^2 + \omega_c^2])}{\bar{\gamma}^2(\Gamma_e^2 + \omega_c^2) + 2\bar{\gamma}\Gamma_{\text{ph}}(\Gamma_e(\bar{\gamma} + \Gamma_e) + \omega_c^2)\bar{w}^2 + \Gamma_{\text{ph}}^2((\bar{\gamma} + \Gamma_e)^2 + \omega_c^2)\bar{w}^4} \right), \quad (\text{D6c})$$

$$T\bar{\kappa}_{yx} \approx \frac{\nu}{2} p_{\text{F}}^2 v_{\text{F}}^4 \left(\frac{\omega_c\bar{a}^2}{\Gamma_e^2 + \omega_c^2 + 2\Gamma_e\bar{\gamma} + \bar{\gamma}^2} + \frac{r^4\bar{w}^4\bar{\gamma}^2\omega_c}{\bar{\gamma}^2(\Gamma_e^2 + \omega_c^2) + 2\bar{\gamma}\Gamma_{\text{ph}}(\Gamma_e(\bar{\gamma} + \Gamma_e) + \omega_c^2)\bar{w}^2 + \Gamma_{\text{ph}}^2((\bar{\gamma} + \Gamma_e)^2 + \omega_c^2)\bar{w}^4} \right), \quad (\text{D6d})$$

$$T\alpha_{xx} \approx -e \frac{\nu}{2} p_{\text{F}} v_{\text{F}}^3 \left(\frac{\bar{\gamma}r^2\bar{w}^2(\bar{\gamma}\Gamma_e + (\bar{\gamma} + \Gamma_e)\Gamma_{\text{ph}}\bar{w}^2)}{\bar{\gamma}^2(\Gamma_e^2 + \omega_c^2) + 2\bar{\gamma}\Gamma_{\text{ph}}(\Gamma_e(\bar{\gamma} + \Gamma_e) + \omega_c^2)\bar{w}^2 + \Gamma_{\text{ph}}^2((\bar{\gamma} + \Gamma_e)^2 + \omega_c^2)\bar{w}^4} + \frac{\bar{a}^2(\Gamma_e + \bar{\gamma})}{\Gamma_e^2 + \omega_c^2 + 2\Gamma_e\bar{\gamma} + \bar{\gamma}^2} \right) \quad (\text{D6e})$$

$$\begin{aligned} & + \frac{\bar{a}}{((\bar{\gamma}_e + \bar{\gamma})^2 + \omega_c^2)((\bar{\gamma}\Gamma_e + \Gamma_{\text{ph}}(\bar{\gamma} + \Gamma_e)\bar{w}^2)^2 + \omega_c^2(\bar{\gamma} + \Gamma_{\text{ph}}\bar{w}^2)^2)} \\ & \times \left\{ (\bar{\gamma} + \Gamma_{\text{ph}}\bar{w}^2) [-c(2\bar{\gamma}\Gamma_e\omega_c + \Gamma_{\text{ph}}(\bar{\gamma} + 2\Gamma_e)\omega_c\bar{w}^2) + b(\bar{\gamma}(-\Gamma_e^2 + \omega_c^2) + \Gamma_{\text{ph}}(-\Gamma_e(\bar{\gamma} + \Gamma_e) + \omega_c^2)\bar{w}^2)] \right. \\ & - \bar{\gamma} [c\omega_c(\bar{\gamma} + \Gamma_{\text{ph}})^2 + b(\bar{\gamma}^2\Gamma_e + \bar{\gamma}\Gamma_{\text{ph}}(\bar{\gamma} + 2\Gamma_e)\bar{w}^2 + \Gamma_{\text{ph}}^2(\bar{\gamma} + \Gamma_e)\bar{w}^4)] \\ & - \bar{a}\bar{\gamma}(2\bar{\gamma} + \Gamma_{\text{ph}}\bar{w}^2) [\bar{\gamma}(-\Gamma_e^2 + \omega_c^2) + \Gamma_{\text{ph}}(-\Gamma_e(\bar{\gamma} + \Gamma_e) + \omega_c^2)\bar{w}^2] \\ & \left. + \bar{a}\bar{\gamma}^2(2\bar{\gamma} + \Gamma_{\text{ph}}\bar{w}^2) [\Gamma_e\Gamma_{\text{ph}}\bar{w}^2 + \bar{\gamma}(\Gamma_e + \Gamma_{\text{ph}}\bar{w}^2)] \right\}, \end{aligned}$$

$$T\alpha_{yx} \approx -e \frac{\nu}{2} p_{\text{F}} v_{\text{F}}^3 \left(\frac{\omega_c\bar{\gamma}r^2\bar{w}^2(\bar{\gamma} + \Gamma_{\text{ph}}\bar{w}^2)}{\bar{\gamma}^2(\Gamma_e^2 + \omega_c^2) + 2\bar{\gamma}\Gamma_{\text{ph}}(\Gamma_e(\bar{\gamma} + \Gamma_e) + \omega_c^2)\bar{w}^2 + \Gamma_{\text{ph}}^2((\bar{\gamma} + \Gamma_e)^2 + \omega_c^2)\bar{w}^4} + \frac{\omega_c\bar{a}^2}{(\Gamma_e^2 + \omega_c^2) + 2\Gamma_e\bar{\gamma} + \bar{\gamma}^2} \right) \quad (\text{D6f})$$

$$\begin{aligned} & + \frac{\bar{a}}{((\Gamma_e + \bar{\gamma})^2 + \omega_c^2)((\bar{\gamma}\Gamma_e + \Gamma_{\text{ph}}(\bar{\gamma} + \Gamma_e)\bar{w}^2)^2 + \omega_c^2(\bar{\gamma} + \Gamma_{\text{ph}}\bar{w}^2)^2)} \\ & \times \left\{ (\bar{\gamma} + \Gamma_{\text{ph}}\bar{w}^2) [-b(2\bar{\gamma}\Gamma_e\omega_c + \Gamma_{\text{ph}}(\bar{\gamma} + 2\Gamma_e)\omega_c\bar{w}^2) - c(\bar{\gamma}(-\Gamma_e^2 + \omega_c^2) + \Gamma_{\text{ph}}(-\Gamma_e(\bar{\gamma} + \Gamma_e) + \omega_c^2)\bar{w}^2)] \right. \\ & - \bar{\gamma} [b\omega_c(\bar{\gamma} + \Gamma_{\text{ph}})^2 - c(\bar{\gamma}^2\Gamma_e + \bar{\gamma}\Gamma_{\text{ph}}(\bar{\gamma} + 2\Gamma_e)\bar{w}^2 + \Gamma_{\text{ph}}^2(\bar{\gamma} + \Gamma_e)\bar{w}^4)] \\ & + \bar{a}\bar{\gamma}\omega_c(2\bar{\gamma} + \Gamma_e\bar{w}^2)(2\bar{\gamma}\Gamma_e + (\bar{\gamma} + 2\Gamma_e)\Gamma_{\text{ph}}\bar{w}^2) \\ & \left. + \bar{a}\bar{\gamma}^2\omega_c(2\bar{\gamma} + \Gamma_{\text{ph}}\bar{w}^2)(\bar{\gamma} + \Gamma_{\text{ph}}\bar{w}^2) \right\}. \end{aligned}$$

Notice that we still keep the leading order in T/T_{F} . All the conductivities above can be checked to reduce to (5.5)

when $B = 0$. The experimental thermal conductivity is given by

$$T\kappa_{xx} \approx \begin{cases} \frac{\nu}{2} p_F^2 v_F^4 \left(\frac{(\bar{a}^2 \Gamma_e + r^2 \gamma)}{\Gamma_e^2 + \omega_c^2 + 2\Gamma_e \gamma r^2 / \bar{a}^2 + \gamma^2 r^4 / \bar{a}^4} + \frac{r^4 \bar{w}^2}{\Gamma_{\text{ph}} + \gamma / \bar{w}^2} \right) & T < T_{\text{BG}} \\ \frac{\nu}{2} p_F^2 v_F^4 \left(\frac{\bar{a}^2 (\Gamma_e + \bar{\gamma})}{\Gamma_e^2 + \omega_c^2 + 2\Gamma_e \bar{\gamma} + \bar{\gamma}^2} + \frac{r^4 \bar{w}^2}{\Gamma_{\text{ph}} + \bar{\gamma} / \bar{w}^2} \right) & T_{\text{BG}} < T \ll T_{\text{F}} \end{cases}, \quad (\text{D7a})$$

$$T\kappa_{yx} \approx \begin{cases} \frac{\nu}{2} p_F^2 v_F^4 \frac{\omega_c \bar{a}^2}{(\Gamma_e^2 + \omega_c^2) + 2\Gamma_e \gamma r^2 / \bar{a}^2 + \gamma^2 r^4 / \bar{a}^4} & T < T_{\text{BG}} \\ \frac{\nu}{2} p_F^2 v_F^4 \frac{\omega_c \bar{a}^2}{\Gamma_e^2 + \omega_c^2 + 2\Gamma_e \bar{\gamma} + \bar{\gamma}^2} & T_{\text{BG}} < T \ll T_{\text{F}} \end{cases}. \quad (\text{D7b})$$

We find that the phonon modes contribute to the non-Hall experimental thermal conductivity in a B -independent way, while do not contribute to the Hall experimental thermal conductivity.

-
- [1] R. N. Gurzhi, “Minimum of resistance in impurity-free conductors,” *Journal of Experimental and Theoretical Physics* **17**, 521 (1963).
- [2] D. A. Bandurin et al., “Negative local resistance caused by viscous electron backflow in graphene,” *Science* **351**, 1055 (2016).
- [3] J. Crossno, J. K. Shi, K. Wang, X. Liu, A. Harzheim, A. Lucas, S. Sachdev, P. Kim, T. Taniguchi, K. Watanabe, and et al., “Observation of the Dirac fluid and the breakdown of the Wiedemann-Franz law in graphene,” *Science* **351**, 1058 (2016).
- [4] Fereshte Ghahari, Hong-Yi Xie, Takashi Taniguchi, Kenji Watanabe, Matthew S. Foster, and Philip Kim, “Enhanced thermoelectric power in graphene: Violation of the mott relation by inelastic scattering,” *Phys. Rev. Lett.* **116**, 136802 (2016).
- [5] R. Krishna Kumar et al., “Superballistic flow of viscous electron fluid through graphene constrictions,” *Nature Physics* **13**, 1182 (2017).
- [6] Patrick Gallagher, Chan-Shan Yang, Tairu Lyu, Fanglin Tian, Rai Kou, Hai Zhang, Kenji Watanabe, Takashi Taniguchi, and Feng Wang, “Quantum-critical conductivity of the dirac fluid in graphene,” *Science* **364**, 158–162 (2019).
- [7] A. I. Berdyugin, S. G. Xu, F. M. D. Pellegrino, R. Krishna Kumar, A. Principi, I. Torre, M. Ben Shalom, T. Taniguchi, K. Watanabe, I. V. Grigorieva, and et al., “Measuring hall viscosity of graphenes electron fluid,” *Science* **364**, 162 (2019).
- [8] J. A. Sulpizio et al, “Visualizing Poiseuille flow of hydrodynamic electrons,” *Nature* **576**, 75 (2019).
- [9] A. Jenkins, S. Baumann, H. Zhou, S. A. Meynell, D. Yang, K. Watanabe, T. Taniguchi, A. Lucas, A. F. Young, and A. C. Bleszynski Jayich, “Imaging the breakdown of ohmic transport in graphene,” (2020), [arXiv:2002.05065](https://arxiv.org/abs/2002.05065) [[cond-mat.mes-hall](https://arxiv.org/abs/2002.05065)].
- [10] Mark J. H. Ku, Tony X. Zhou, Qing Li, Young J. Shin, Jing K. Shi, Claire Burch, Laurel E. Anderson, Andrew T. Pierce, Yonglong Xie, Assaf Hamo, and et al., “Imaging viscous flow of the dirac fluid in graphene,” *Nature* **583**, 537541 (2020).
- [11] M. J. M. de Jong and L. W. Molenkamp, “Hydrodynamic electron flow in high-mobility wires,” *Physical Review B* **51**, 13389 (1995).
- [12] G. M. Gusev, A. D. Levin, E. V. Levinson, and A. K. Bakarov, “Viscous electron flow in mesoscopic two-dimensional electron gas,” *AIP Advances* **8**, 025318 (2018).
- [13] Andrew Lucas and Kin Chung Fong, “Hydrodynamics of electrons in graphene,” *Journal of Physics: Condensed Matter* **30**, 053001 (2018).
- [14] Haoyu Guo, Ekin Ilseven, Gregory Falkovich, and Leonid S. Levitov, “Higher-than-ballistic conduction of viscous electron flows,” *Proceedings of the National Academy of Sciences* **114**, 30683073 (2017).
- [15] Leonid Levitov and Gregory Falkovich, “Electron viscosity, current vortices and negative nonlocal resistance in graphene,” *Nature Physics* **12**, 672676 (2016).
- [16] Iacopo Torre, Andrea Tomadin, Andre K. Geim, and Marco Polini, “Nonlocal transport and the hydrodynamic shear viscosity in graphene,” *Physical Review B* **92**, 165433 (2015).
- [17] P. S. Alekseev, “Negative magnetoresistance in viscous flow of two-dimensional electrons,” *Phys. Rev. Lett.* **117**, 166601 (2016).
- [18] A. V. Andreev, Steven A. Kivelson, and B. Spivak, “Hydrodynamic description of transport in strongly correlated electron systems,” *Physical Review Letters* **106**, 256804 (2011).
- [19] S. S. Apostolov, A. Levchenko, and A. V. Andreev, “Hydrodynamic coulomb drag of strongly correlated electron liquids,” *Physical Review B* **89**, 121104 (2014).
- [20] Davide Forcella, Jan Zaanen, Davide Valentini, and Dirk van der Marel, “Electromagnetic properties of viscous charged fluids,” *Physical Review B* **90**, 035143 (2014).
- [21] Andrea Tomadin, Giovanni Vignale, and Marco Polini, “Corbino disk viscometer for 2d quantum electron liquids,” *Physical Review Letters* **113**, 235901 (2014).
- [22] Uri Vool, Assaf Hamo, Georgios Varnavides, Yaxian Wang, Tony X. Zhou, Nitesh Kumar, Yuliya Dovzhenko, Ziwei Qiu,

- Christina A. C. Garcia, Andrew T. Pierce, Johannes Gooth, Polina Anikeeva, Claudia Felser, Prineha Narang, and Amir Yacoby, “Imaging phonon-mediated hydrodynamic flow in wte2 with cryogenic quantum magnetometry,” (2020), [arXiv:2009.04477 \[cond-mat.mes-hall\]](#).
- [23] J. Gooth, F. Menges, N. Kumar, V. Suss, C. Shekhar, Y. Sun, U. Drechsler, R. Zierold, C. Felser, and B. Gotsmann, “Thermal and electrical signatures of a hydrodynamic electron fluid in tungsten diphosphide,” *Nature Communications* **9**, 4093 (2018).
- [24] Jennifer Coulter, Ravishankar Sundararaman, and Prineha Narang, “Microscopic origins of hydrodynamic transport in the type-ii weyl semimetal wp_2 ,” *Phys. Rev. B* **98**, 115130 (2018).
- [25] Gavin B. Osterhoudt, Vincent M. Plisson, Yaxian Wang, Christina A. C. Garcia, Johannes Gooth, Claudia Felser, Prineha Narang, and Kenneth S. Burch, “Evidence for dominant phonon-electron scattering in weyl semimetal wp_2 ,” (2020), [arXiv:2007.10364 \[cond-mat.mtrl-sci\]](#).
- [26] Chenguang Fu, Thomas Scaffidi, Jonah Weissman, Yan Sun, Rana Saha, Sarah J. Watzman, Abhay K. Srivastava, Guowei Li, Walter Schnelle, Peter Werner, Machteld E. Kamminga, Subir Sachdev, Stuart S. P. Parkin, Sean A. Hartnoll, Claudia Felser, and Johannes Gooth, “Thermoelectric signatures of the electron-phonon fluid in ptn_4 ,” (2018), [arXiv:1802.09468 \[cond-mat.mtrl-sci\]](#).
- [27] P. J. W. Moll, P. Kushwaha, N. Nandi, B. Schmidt, and A. P. Mackenzie, “Evidence for hydrodynamic electron flow in $PdCoO_2$,” *Science* **351**, 1061 (2016).
- [28] Caleb Q. Cook and Andrew Lucas, “Electron hydrodynamics with a polygonal fermi surface,” *Phys. Rev. B* **99**, 235148 (2019).
- [29] M. S. Steinberg, “Viscosity of the electron gas in metals,” *Phys. Rev.* **109**, 1486–1492 (1958).
- [30] H. Nielsen and B. I. Shlosvkii, “Heat transfer and second sound in dielectrics at large drift velocities of the phonon gas,” *Soviet Physics JETP* **29**, 386 (1969).
- [31] R. N. Gurzhi and A. I. Kopeliovich, “Electric conductivity of metals with account of phonon drag,” *Soviet Physics JETP* **34**, 1345 (1972).
- [32] Alex Levchenko and Jrg Schmalian, “Transport properties of strongly coupled electron-phonon liquids,” (2020), [arXiv:2005.09694 \[cond-mat.mes-hall\]](#).
- [33] E. H. Hwang and S. Das Sarma, “Limit to two-dimensional mobility in modulation-doped gaas quantum structures: How to achieve a mobility of 100 million,” *Phys. Rev. B* **77**, 235437 (2008).
- [34] Marco Bernardi, Derek Vigil-Fowler, Chin Shen Ong, Jeffrey B. Neaton, and Steven G. Louie, “Ab initio study of hot electrons in gaas,” *Proceedings of the National Academy of Sciences* **112**, 5291–5296 (2015).
- [35] Dmitri K. Efetov and Philip Kim, “Controlling electron-phonon interactions in graphene at ultrahigh carrier densities,” *Phys. Rev. Lett.* **105**, 256805 (2010).
- [36] S.A. Hartnoll, A. Lucas, and S. Sachdev, *Holographic Quantum Matter*, The MIT Press (MIT Press, 2018).
- [37] Rudolf Baier, Paul Romatschke, Dam Thanh Son, Andrei O. Starinets, and Mikhail A. Stephanov, “Relativistic viscous hydrodynamics, conformal invariance, and holography,” *JHEP* **04**, 100 (2008), [arXiv:0712.2451 \[hep-th\]](#).
- [38] Ali Lavasani, Daniel Bulmash, and Sankar Das Sarma, “Wiedemann-franz law and fermi liquids,” *Phys. Rev. B* **99**, 085104 (2019).
- [39] Andrew Lucas, “Sound waves and resonances in electron-hole plasma,” *Phys. Rev. B* **93**, 245153 (2016).
- [40] Thomas Scaffidi, Nabhanila Nandi, Burkhard Schmidt, Andrew P. Mackenzie, and Joel E. Moore, “Hydrodynamic electron flow and hall viscosity,” *Phys. Rev. Lett.* **118**, 226601 (2017).
- [41] Andrew Lucas and Sankar Das Sarma, “Electronic hydrodynamics and the breakdown of the wiedemann-franz and mott laws in interacting metals,” *Phys. Rev. B* **97**, 245128 (2018).
- [42] Andrew Lucas, “Kinetic theory of electronic transport in random magnetic fields,” *Phys. Rev. Lett.* **120**, 116603 (2018).
- [43] Andrew Lucas and Sean A. Hartnoll, “Kinetic theory of transport for inhomogeneous electron fluids,” *Phys. Rev. B* **97**, 045105 (2018).
- [44] Alex Kamenev, *Field Theory of Non-Equilibrium Systems* (Cambridge University Press, 2011).
- [45] Feliciano Giustino, “Electron-phonon interactions from first principles,” *Rev. Mod. Phys.* **89**, 015003 (2017).
- [46] J.M. Ziman, *Electrons and Phonons: The Theory of Transport Phenomena in Solids*, International series of monographs on physics (OUP Oxford, 2001).
- [47] Maxim Trushin, “Collinear scattering of photoexcited carriers in graphene,” *Phys. Rev. B* **94**, 205306 (2016).
- [48] Lars Fritz, Jörg Schmalian, Markus Müller, and Subir Sachdev, “Quantum critical transport in clean graphene,” *Phys. Rev. B* **78**, 085416 (2008).
- [49] Sean A. Hartnoll, “Theory of universal incoherent metallic transport,” *Nature Physics* **11** (2015), 10.1038/nphys3174.
- [50] Sean A. Hartnoll, Pavel K. Kovtun, Markus Muller, and Subir Sachdev, “Theory of the Nernst effect near quantum phase transitions in condensed matter, and in dyonic black holes,” *Phys. Rev. B* **76**, 144502 (2007), [arXiv:0706.3215 \[cond-mat.str-el\]](#).
- [51] Andrew Lucas, Jesse Crossno, Kin Chung Fong, Philip Kim, and Subir Sachdev, “Transport in inhomogeneous quantum critical fluids and in the dirac fluid in graphene,” *Phys. Rev. B* **93**, 075426 (2016).
- [52] Markus Müller and Subir Sachdev, “Collective cyclotron motion of the relativistic plasma in graphene,” *Phys. Rev. B* **78**, 115419 (2008).
- [53] Tsuneya Ando, Alan B. Fowler, and Frank Stern, “Electronic properties of two-dimensional systems,” *Rev. Mod. Phys.* **54**, 437–672 (1982).
- [54] E. H. Hwang and S. Das Sarma, “Dielectric function, screening, and plasmons in two-dimensional graphene,” *Phys. Rev. B* **75**, 205418 (2007).

- [55] S. Das Sarma and E. H. Hwang, “Collective modes of the massless dirac plasma,” *Phys. Rev. Lett.* **102**, 206412 (2009).
- [56] Trung V. Phan, Justin C. W. Song, and Leonid S. Levitov, “Ballistic heat transfer and energy waves in an electron system,” (2013), [arXiv:1306.4972 \[cond-mat.mes-hall\]](#).
- [57] Sašo Grozdanov, Andrew Lucas, and Napat Poovuttikul, “Holography and hydrodynamics with weakly broken symmetries,” *Phys. Rev. D* **99**, 086012 (2019), [arXiv:1810.10016 \[hep-th\]](#).
- [58] Luca V. Delacrétaz and Andrey Gromov, “Transport signatures of the hall viscosity,” *Phys. Rev. Lett.* **119**, 226602 (2017).
- [59] Francesco M. D. Pellegrino, Iacopo Torre, and Marco Polini, “Nonlocal transport and the hall viscosity of two-dimensional hydrodynamic electron liquids,” *Phys. Rev. B* **96**, 195401 (2017).
- [60] Eundeok Mun, Hyunjin Ko, Gordon J. Miller, German D. Samolyuk, Sergey L. Bud’ko, and Paul. C. Canfield, “Magnetic field effects on transport properties of PtSn_4 ,” *Phys. Rev. B* **85**, 035135 (2012).
- [61] E. H. Hwang and S. Das Sarma, “Linear-in- t resistivity in dilute metals: A fermi liquid perspective,” *Phys. Rev. B* **99**, 085105 (2019).
- [62] M. P. Lilly, J. L. Reno, J. A. Simmons, I. B. Spielman, J. P. Eisenstein, L. N. Pfeiffer, K. W. West, E. H. Hwang, and S. Das Sarma, “Resistivity of dilute 2d electrons in an undoped gaas heterostructure,” *Phys. Rev. Lett.* **90**, 056806 (2003).
- [63] Hryhoriy Polshyn, Matthew Yankowitz, Shaowen Chen, Yuxuan Zhang, K. Watanabe, T. Taniguchi, Cory R. Dean, and Andrea F. Young, “Large linear-in-temperature resistivity in twisted bilayer graphene,” *Nature Physics* **15**, 10111016 (2019).
- [64] S. V. Kravchenko, Whitney E. Mason, G. E. Bowker, J. E. Furneaux, V. M. Pudalov, and M. D’Iorio, “Scaling of an anomalous metal-insulator transition in a two-dimensional system in silicon at $b=0$,” *Phys. Rev. B* **51**, 7038–7045 (1995).
- [65] Georgios Varnavides, Adam S. Jermyn, Polina Anikeeva, Claudia Felser, and Prineha Narang, “Generalized electron hydrodynamics, vorticity coupling, and hall viscosity in crystals,” (2020), [arXiv:2002.08976 \[cond-mat.mtrl-sci\]](#).